

Review

# Recent Advances of Emerging Organic Pollutants Degradation in Environment by Non-Thermal Plasma Technology: A Review

Yongjian He, Wenjiao Sang \*, Wei Lu, Wenbin Zhang, Cheng Zhan and Danni Jia

School of Civil Engineering and Architecture, Wuhan University of Technology, Wuhan 430070, China; hyjwhut@126.com (Y.H.); wluemail@163.com (W.L.); zhangwenbin1114@126.com (W.Z.); wlzhancheng@126.com (C.Z.); jdnwz9998@163.com (D.J.)

\* Correspondence: whlgdxswj@126.com

**Abstract:** Emerging organic pollutants (EOPs), including endocrine disrupting compounds (EDCs), pharmaceuticals and personal care products (PPCPs), and persistent organic pollutants (POPs), constitute a problem in the environmental field as they are difficult to completely degrade by conventional treatment methods. Non-thermal plasma technology is a novel advanced oxidation process, which combines the effects of free radical oxidation, ozone oxidation, ultraviolet radiation, shockwave, etc. This paper summarized and discussed the research progress of non-thermal plasma remediation of EOPs-contaminated water and soil. In addition, the reactive species in the process of non-thermal plasma degradation of EOPs were summarized, and the degradation pathways and degradation mechanisms of EOPs were evaluated of selected EOPs for different study cases. At the same time, the effect of non-thermal plasma in synergy with other techniques on the degradation of EOPs in the environment was evaluated. Finally, the bottleneck problems of non-thermal plasma technology are summarized, and some suggestions for the future development of non-thermal plasma technology in the environmental remediation were presented. This review contributes to our better understanding of non-thermal plasma technology for remediation of EOPs-contaminated water and soil, hoping to provide reference for relevant practitioners.

**Keywords:** advanced oxidation processes; discharge plasma; reactive species; environmental remediation; combination system; degradation mechanism



**Citation:** He, Y.; Sang, W.; Lu, W.; Zhang, W.; Zhan, C.; Jia, D. Recent Advances of Emerging Organic Pollutants Degradation in Environment by Non-Thermal Plasma Technology: A Review. *Water* **2022**, *14*, 1351. <https://doi.org/10.3390/w14091351>

Academic Editors: Dionysios (Dion) Demetriou Dionysiou, Yujue Wang and Huijiao Wang

Received: 29 March 2022

Accepted: 19 April 2022

Published: 21 April 2022

**Publisher's Note:** MDPI stays neutral with regard to jurisdictional claims in published maps and institutional affiliations.



**Copyright:** © 2022 by the authors. Licensee MDPI, Basel, Switzerland. This article is an open access article distributed under the terms and conditions of the Creative Commons Attribution (CC BY) license (<https://creativecommons.org/licenses/by/4.0/>).

## 1. Introduction

Over the past few decades, increasing industrial, agricultural, and human activities have promoted the use of chemicals [1,2]. In addition, the development of human society and the wrong understanding of personal safety have increased the chemical load in water and soil environment. In many developing countries, untreated sewage is also used for agricultural purposes, resulting in substandard or untreated wastewater that adds many pollutants to the food chain [3,4]. Therefore, appropriate technologies are needed to eliminate pollutants in water and soil environment for the sake of protection for both human health and the environment.

Emerging organic pollutants (EOPs) are a kind of organic pollutants which have no environmental monitoring standards or emission standards and have negative effects on ecology and human health [5]. EOPs include endocrine disrupting compounds (EDCs), pharmaceutical and personal care products (PPCPs), and persistent organic pollutants (POPs) [6,7]. EOPs may be candidates for future regulation because of their potential risks to the environment and human health, the continuous entry into the environment and the fact that even the most modern wastewater treatment plants (WWTPs) cannot completely convert/remove these compounds [8]. In recent years, with the improvement of environmental analysis, these substances have been frequently detected in the environment, such as sewage, surface water, drinking water [9], and soil [10]. The continuous detection

of EOPs brings new challenges to environmental pollution control and makes the treatment of EOPs become an international research hotspot.

Currently, there are many methods for organic pollutants degradation in water environment: bioremediation [11,12], advanced oxidation processes (AOPs) [13–15], adsorption process [16,17], membrane treatment [18,19], and combination process [20]. Compared with water remediation, organic pollution in soil is so subtle that it is difficult to detect. In addition, soil remediation tends to be costlier and takes longer to complete. Therefore, it is urgent to develop effective and convenient remediation technology for organic contaminated soil. At present, many methods have been developed for different organic contaminated soils, including physical remediation (e.g., thermal desorption [21], soil vapor extraction [22]), chemical remediation (e.g., soil washing [23], electrochemical remediation [24], chemical oxidation remediation [25]), and biological remediation (e.g., microbial remediation [26], phytoremediation [27]). With the exception of AOPs, most of these technologies either transfer contaminants from one phase to another rather than complete degradation and mineralization, or are not efficient when the concentration of organic pollutants is at low levels. However, bioremediation often requires long treatment time and it is difficult to reduce the pollution level below the standard.

Non-thermal plasma may be a viable alternative to more common AOPs due to its comparable energy requirements for contaminant degradation and its ability to operate without any additional chemicals [28]. Non-thermal plasma technology has been used as a method to degrade EOPs, including EDCs [29,30] (e.g., pesticides, industrial chemicals, steroids), PPCPs [31–34] (e.g., antibiotics, antidepressant, anti-inflammatories, antimicrobials, surfactants), and POPs [35,36] (e.g., polychlorinated biphenyls, polycyclic aromatic hydrocarbons, organochlorine pesticides). In the review of Magureanu et al. [37], research on the degradation of various pharmaceutical compounds by non-thermal plasma was discussed, and the removal efficiency of target compounds and the energy yield of plasma technology were compared and discussed. Russo et al. [38] summarized the research works on the removal and mineralization of organic pollutants in water by the combination of non-thermal plasma and catalyst. They concluded that the catalyst played an important role in improving the performance of the plasma system. Zhang et al. [39] introduced several typical non-thermal plasma sources for remediation of organic contaminated soil. The effects of different important parameters (such as applied voltage, reactor configuration, soil properties, type of feed air, and gas flow rate) on the remediation performance were discussed. Guo et al. [40] supplemented the research on the mechanism and process of repairing organic contaminated soil by discharge plasma on the basis of previous reviews. Figure 1 shows bibliography data of papers related to non-thermal plasma technology for the degradation of pollutants published in the last decade. As shown in Figure 1a, the number of published papers using non-thermal plasma as a means of pollutant degradation in the last decade has always maintained high and is gradually increasing. Especially, PPCPs and POPs have become hotspots in this field (as shown in Figure 1b).

During the past decade, a number of studies have reported the degradation of EOPs in the environment by non-thermal plasma. At present, the review of non-thermal plasma mainly focuses on water remediation [41–45], and a few reviews have also summarized its application in soil remediation [39,40], but there is a lack of comprehensive review on water and soil remediation. Therefore, this paper focuses on the degradation of different types of EOPs (i.e., EDCs, PPCPs, and POPs) in water and soil environment by the non-thermal plasma technology. Since the reactive species in the plasma system play an indispensable role in the degradation of pollutants, the generation of reactive species in non-thermal plasma is reviewed. In addition, this review also summarizes the research progress of degradation pathways of different kinds of EOPs by non-thermal plasma. An important part of this work is devoted to the combination of non-thermal plasma with various other technologies to compensate for the shortcomings of plasmas alone. In this review, the bottleneck problems of non-thermal plasma and the future prospects are also presented.

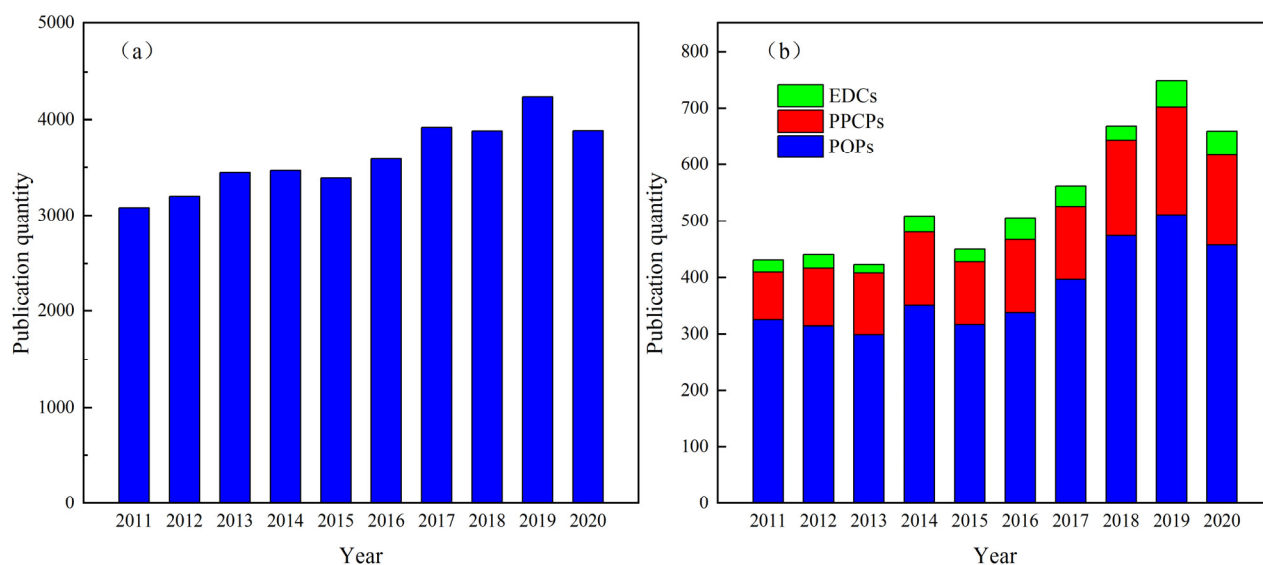


**Figure 1.** Statistics of papers about non-thermal plasma technology as a method for the degradation of (a) pollutants and (b) EOPs (EDCs, PPCPs, and POPs) published in the last ten years (data obtained from Web of Science).

## 2. Degradation of Emerging Organic Pollutants by Non-Thermal Plasma Technology

Different kinds of EOPs may cause harm to human health and ecological environment; so, it is necessary to find appropriate methods to deal with EOPs. EDCs, also known as environmental hormones, can bind to hormone receptors in organisms and disrupt normal metabolism in the endocrine system [46]. Many researchers have reported their toxic effects on human health and the environment [47]. PPCPs are the most widely used chemical reagents in animal husbandry, agriculture, and human daily life. However, they have the potential to cause serious ecotoxicological problems and pose a great threat to ecosystems or organisms [48–50]. It is worth mentioning that antibiotics with a certain concentration level in the environment for a long time may not only have toxic effects on some sensitive organisms, but also lead to the generation, maintenance, transfer and transmission of antibiotic-resistant bacteria (ARB), and antibiotic resistance genes (ARGs) under selective pressure [51]. Since the adoption of the “Stockholm Convention” by the United Nations Environment Program (UNEP) in 2001, awareness of the potential risks of POPs in the environment and the need to remove POPs from the environment have become more urgent. POPs are generally considered to have three basic physical and chemical properties: persistence, lipophilicity, and long-distance mobility. These properties enable them to perform bioamplification and bioaccumulation in animals and seriously harm the health of humans and the natural environment. Therefore, it is imperative to develop environmentally friendly removal methods. Faced with this environmental problem, many researchers have focused on AOPs to eliminate EOPs that are resistant to conventional treatment processes [52–54]. Non-thermal plasma may be a viable alternative to more common AOPs due to its comparable energy requirements for contaminant degradation and its ability to operate without any additional chemicals. The specific research results of non-thermal plasma in water and soil remediation are introduced below.

### 2.1. Water Remediation

Researchers have paid extensive attention to the degradation of EOPs in recent years and, in order to reduce the risk of EOPs in water environment, non-thermal plasma has been a widely studied and applied technology. Summaries of some representative studies are compiled in Table 1.

**Table 1.** Overview of work done in the degradation of EOPs in water by non-thermal plasma.

| EDCs                          |                                     |  |   |      |
|-------------------------------|-------------------------------------|--|---|------|
| Target Compounds              | Non-Thermal Plasma System           | Experimental Condition   | Results   | Ref. |
| 17 $\alpha$ -ethinylestradiol | Corona discharge plasma             | Discharge voltage: 16 kV;<br>Frequency: 20 Hz;<br>Solution volume: 100 mL;<br>Initial concentration: 100 $\mu$ g/L   | Degradation efficiency: ~100% (0.25 min);<br>Energy yield: 4.80 g/kWh   | [55] |
| Bisphenol A                   | Pulsed discharge plasma             | Discharge voltage: 20 kV;<br>Frequency: 50 Hz;<br>Air flow rate: 4.0 L/min;<br>Initial concentration: 20 mg/L  | Degradation efficiency: 75.1% (60 min);<br>TOC removal efficiency: 29.8%  | [56] |
| Bisphenol A                   | Dielectric barrier discharge plasma | Discharge voltage: 5 kV;<br>Gas flow rate: 0.5 L/min;<br>Solution volume: 500 mL;<br>Initial concentration: 20 mg/L  | Degradation efficiency: 67.8% (60 min);<br>TOC removal efficiency: 34.2%  | [57] |
| Bisphenol A                   | Dielectric barrier discharge plasma | Discharge voltage: 5 kV;<br>Gas flow rate: 0.5 L/min;<br>Solution volume: 500 mL;<br>Initial concentration: 20 mg/L  | Degradation efficiency: 69.5% (60 min);<br>Energy yield: 0.117 g/kWh  | [58] |
| Bisphenol A                   | Dielectric barrier discharge plasma | Discharge voltage: 16.8 kV;<br>Discharge power: 412.5 W;<br>Solution volume: 500 mL;<br>Initial concentration: 50 mg/L;<br>Initial pH = 6  | Degradation efficiency: 100% (25 min);<br>Rate constant: 0.152 min <sup>-1</sup>                                | [59] |
| P-methylphenol                | Dielectric barrier discharge plasma | Discharge voltage: 110 V;<br>O <sub>2</sub> flow rate: 100 mL/min;<br>Liquid flow rate: 100 mL/min;<br>Solution volume: 400 mL;<br>Initial concentration: 100 mg/L;<br>Initial pH: 6.1 | Degradation efficiency: 49.13% (8 min)  | [60] |
| Dichlorvos                    |                                     | Discharge voltage: 80 kV;<br>Solution volume: 20 mL;<br>Frequency: 50 Hz;<br>Initial concentration: 850 ppb  | Degradation efficiency: 78.98% (8 min);<br>Rate constant: 0.00303 s <sup>-1</sup>                               |      |
| Malathion                     | Dielectric barrier discharge plasma | Discharge voltage: 80 kV;<br>Solution volume: 20 mL;<br>Frequency: 50 Hz;<br>Initial concentration: 1320 ppb   | Degradation efficiency: 69.62% (8 min);<br>Rate constant: 0.00239 s <sup>-1</sup>                               | [61] |
| Endosulfan                    |                                     | Discharge voltage: 80 kV;<br>Solution volume: 20 mL;<br>Frequency: 50 Hz;<br>Initial concentration: 350 ppb  | Degradation efficiency: 57.71% (8 min);<br>Rate constant: 0.00192 s <sup>-1</sup>                               |      |
| Dimethyl phthalate            | Dielectric barrier discharge plasma | Discharge voltage: 18 kV;<br>Air flow rate: 2.5 L/min;<br>Solution volume: 500 mL;<br>Initial concentration: 30 mg/L   | Degradation efficiency: 61.4% (30 min);<br>Rate constant: 0.029 min <sup>-1</sup> ;<br>Energy yield: 0.29 g/kWh | [62] |
| 4-chlorophenol                | Corona discharge plasma             | Discharge voltage: 20 kV;<br>Frequency: 100 Hz;<br>Flow rate: 200 mL/min;<br>Solution volume: 200 mL;<br>Initial concentration: 100 mg/L   | Degradation efficiency: 86.2% (40 min);   | [63] |

Table 1. Cont.

| PPCPs            |                                     |   |   |      |
|------------------|-------------------------------------|---|---|------|
| Target Compounds | Non-Thermal Plasma System           | Experimental Condition  | Results   | Ref. |
| Enrofloxacin     | Pulsed discharge plasma             | Discharge voltage: 20 kV;<br>Frequency: 50 Hz;<br>Air flow rate: 4 L/min;<br>Solution volume: 150 mL;<br>Initial concentration: 20 mg/L                             | Degradation efficiency: 76% (60 min);<br>Energy yield: 18.7 mg/kJ   | [64] |
| Tetracycline     | Surface discharge plasma            | Discharge voltage: 7 kV;<br>Frequency: 6 kHz;<br>Air flow rate: 1.0 L/min;<br>Solution volume: 900 mL;<br>Initial concentration: 40 mg/L                            | Degradation efficiency: 82.6% (15 min);<br>Energy yield: 16.1 mg/kJ   | [65] |
| Pefloxacin       | Dielectric barrier discharge plasma | Discharge power: 0.7 W;<br>Frequency: 50 Hz;<br>O <sub>2</sub> flow rate: 125 mL/min;<br>Solution volume: 100 mL;<br>Initial concentration: 120 mg/L                | Degradation efficiency: 96.1% (25 min);<br>Energy yield: 39.6 g/kWh   | [66] |
| Oxytetracycline  | Dielectric barrier discharge plasma | Discharge voltage: 4.8 kV;<br>Frequency: 10 kHz;<br>Air flow rate: 1.0 L/min;<br>Solution volume: 200 mL;<br>Initial concentration: 50 mg/L                         | Degradation efficiency: 88.2% (20 min);<br>TOC removal efficiency: 36.7%;<br>COD removal efficiency: 21.2%;<br>Energy yield: 0.27 mg/kJ | [67] |
| Amoxicillin      | Dielectric barrier discharge plasma | Discharge voltage: 15 kV;<br>Frequency: 50 Hz;<br>Initial concentration: 16 mg/L;<br>Initial pH: 4.5  | Degradation efficiency: 75% (18 min)  | [68] |
| Chloramphenicol  | Pulsed discharge plasma             | Discharge voltage: 19 kV;<br>Air flow rate: 4 L/min;<br>Solution volume: 150 mL;<br>Initial concentration: 20 mg/L;<br>Initial pH: 6.9                              | Degradation efficiency: ~45% (60 min);<br>Energy yield: 10.77 mg/kWh  | [69] |
| Tetracycline     | Dielectric barrier discharge plasma | Discharge voltage: 7 kV;<br>Discharge power: 38.8 W;<br>Air flow rate: 2.0 L/min;<br>Solution volume: 450 mL;<br>Initial concentration: 50 mg/L;<br>Initial pH: 7.2 | Degradation efficiency: ~52% (5 min);<br>Energy yield: 3.79 g/kWh   | [70] |
| Ofloxacin        | Pulsed discharge plasma             | Discharge voltage: 18 kV;<br>Solution volume: 150 mL;<br>Initial concentration: 20 mg/L   | Degradation efficiency: 65.0% (60 min);<br>Rate constant: 0.017 min <sup>-1</sup>   | [71] |
| Oxytetracycline  | Pulsed discharge plasma             | Discharge voltage: 18 kV;<br>Air flow rate: 4 L/min;<br>Solution volume: 150 mL;<br>Initial concentration: 40 mg/L;<br>Initial pH: 3.2                              | Degradation efficiency: 59% (60 min);<br>TOC removal efficiency: 23.8%  | [72] |
| Acetaminophen    | Dielectric barrier discharge plasma | Discharge voltage: 18 kV;<br>Air flow rate: 200 L/h;<br>Solution volume: 180 mL;<br>Initial concentration: 20 ppm   | Degradation efficiency: 50% (18 min)  | [73] |

Table 1. Cont.

| PPCPs            |                                     |  |   |      |
|------------------|-------------------------------------|--|---|------|
| Target Compounds | Non-Thermal Plasma System           | Experimental Condition   | Results   | Ref. |
| Diclofenac       | Dielectric barrier discharge plasma | Discharge power: 150 W;<br>Ar flow rate: 20 L/h;<br>Solution volume: 500 mL;<br>Initial concentration: 50 mg/L;<br>Initial pH: 5.6;  | Degradation efficiency: 100%<br>(30 min)  | [74] |
| Ibuprofen        |                                     | Discharge power: 150 W;<br>Ar flow rate: 20 L/h;<br>Solution volume: 500 mL;<br>Initial concentration: 50 mg/L;<br>Initial pH: 5.7;  | Degradation efficiency: 100%<br>(20 min)  |      |
| Ibuprofen        | Corona discharge plasma             | Discharge voltage: 18 kV;<br>Discharge power: 2.1 W;<br>Frequency: 25 Hz;<br>Solution volume: 330 mL;<br>Initial concentration: 22.8 mg/L  | Degradation efficiency: 100%<br>(20 min);<br>Energy yield: 20.2 g/kWh   | [75] |
| Ibuprofen        | Dielectric barrier discharge plasma | Discharge power: 70 W;<br>Air flow rate: 0.50 m <sup>3</sup> /h;<br>Initial concentration: 18 mg/L;<br>Initial pH: 6.72  | Degradation efficiency: 95.6%<br>(5 min)  | [76] |
| Diclofenac       | Corona discharge plasma             | Discharge voltage: 80 kV;<br>Frequency: 20 Hz;<br>Solution volume: 300 mL;<br>Initial concentration: 0.5 mg/L  | Degradation efficiency: >80%<br>(15 min)  | [77] |
| Amoxicillin      | Dielectric barrier discharge plasma | Discharge power: ~2 W;<br>O <sub>2</sub> flow rate: 600 sccm;<br>Solution volume: 200 mL;<br>Initial concentration: 100 mg/L;<br>Initial pH: 8                                     | Degradation efficiency: ~100%<br>(10 min)   | [78] |
| Oxacillin        |                                     |  | Degradation efficiency: ~100%<br>(30 min)   |      |
| Ampicillin       |                                     |  | Degradation efficiency: ~100%<br>(30 min)   |      |
| Diclofenac       | Pulsed corona discharge plasma      | Discharge voltage: 18 kV;<br>Frequency: 22 Hz;<br>O <sub>2</sub> flow rate: 1 L/min;<br>Solution volume: 55 mL;<br>Initial concentration: 50 mg/L                                  | Degradation efficiency: 100%<br>(15 min);<br>TOC removal efficiency: 50%<br>(30 min)                                | [79] |
| Enalapril        | Dielectric barrier discharge plasma | Discharge voltage: 18 kV;<br>Discharge power: 2 W<br>Frequency: 50 Hz;<br>O <sub>2</sub> flow rate: 600 sccm;<br>Solution volume: 300 mL;<br>Initial concentration: 50 mg/L        | Degradation efficiency: ~90%<br>(15 min);<br>TOC removal efficiency: >40%<br>(120 min);<br>Energy yield: 4.33 g/kWh | [80] |
| Paracetamol      | Dielectric barrier discharge plasma | Discharge voltage: 5.9 kV;<br>Frequency: 500 Hz;<br>Air flow rate: 100 sccm;<br>Solution volume: 40 mL;<br>Initial concentration: 25 mg/L  | Degradation efficiency: 90%<br>(60 min);<br>Energy yield: 2.9 g/kWh   | [81] |
| Verapamil        | Dielectric barrier discharge plasma | Discharge voltage: 18 kV;<br>Frequency: 50 Hz;<br>N <sub>2</sub> :O <sub>2</sub> = 80:20;<br>Gas flow rate: 30 mL/min;<br>Solution volume: 70 mL;<br>Initial concentration: 0.1 mM | Degradation efficiency: >99%<br>(40 min)  | [82] |



Table 1. Cont.

| PPCPs                         |                                     |   |  |      |
|-------------------------------|-------------------------------------|---|--|------|
| Target Compounds              | Non-Thermal Plasma System           | Experimental Condition  | Results  | Ref. |
| Dimethyl phthalate            | Liquid phase plasma                 | Discharge voltage: 250 V;<br>Frequency: 30 kHz;<br>Solution volume: 600 mL;<br>Initial concentration: 20 ppm  | Degradation efficiency: 63%<br>(180 min);<br>Rate constant: 0.00433 min <sup>-1</sup>                      | [83] |
| Caffeine                      | Dielectric barrier discharge plasma | Discharge power: 60 W;<br>Frequency: 10 kHz;<br>Solution volume: 20 mL;<br>Initial concentration: 100 µg/mL   | Degradation efficiency: 72.6%<br>(4 min)   | [84] |
| Caffeine                      | Dielectric barrier discharge plasma | Discharge power: 75 W;<br>Solution volume: 100 mL;<br>Initial concentration: 50 mg/L  | Degradation efficiency: 41%<br>(24 min);<br>TOC removal efficiency: >10%                                   | [85] |
| Perfluorooctanoic acid        | Dielectric barrier discharge plasma | Discharge voltage: 22 kV;<br>Solution volume: 250 mL;<br>Initial concentration: 20 mg/L   | Degradation efficiency: 73.5%<br>(60 min);<br>TOC removal efficiency: 28.9%;<br>Energy yield: 46.39 mg/kWh | [86] |
| Diatrizoate                   | Corona discharge plasma             | Discharge voltage: 11 kV;<br>Frequency: 3 kHz;<br>Solution volume: 7.5 mL;<br>Initial concentration: 200 µg/L   | Degradation efficiency: 90%<br>(20 min);<br>Energy yield: 0.140 g/kWh                                      | [87] |
| Pentoxifylline                | Dielectric barrier discharge plasma | Discharge voltage: 12 kV;<br>Frequency: 120 Hz;<br>O <sub>2</sub> flow rate: 600 sccm;<br>Solution volume: 200 mL;<br>Initial concentration: 100 mg/L;<br>Initial pH: 7 | Degradation efficiency: 92.5%<br>(60 min);<br>Energy yield: 16 g/kWh                                       | [88] |
| Carbamazepine                 | Dielectric barrier discharge plasma | Discharge voltage: 8 kV;<br>Frequency: 500 Hz;<br>Initial concentration: 0.219 µg/L   | Degradation efficiency: 90%  | [28] |
| POPs                          |                                     |   |  |      |
| Target Compounds              | Non-Thermal Plasma system           | Experimental Condition  | Results  | Ref. |
| 3,3',4,4'-tetrachlorobiphenyl | Dielectric barrier discharge plasma | Discharge voltage: 10 kV;<br>Feed gas: He;<br>Solution volume: 3 mL;<br>Initial concentration: 0.2 mM   | Degradation efficiency: 80% (2 min)  | [89] |
| 2,2',4,4'-tetrachlorobiphenyl | Pulsed corona discharges plasma     | Discharge voltage: 45 kV;<br>Frequency: 60 Hz;<br>Initial conductivity: 100 µs/cm;<br>Initial concentration: 68 ppb   | Degradation efficiency: 70%<br>(60 min)  | [90] |

Non-thermal plasma technology has been proved to be an effective method to degrade EOPs in water environment. For example, Yang et al. [59] studied the degradation of bisphenol A (BPA) in water by dielectric barrier discharge (DBD) plasma. The results showed that BPA was completely degraded (100%) within 25 min when the discharge voltage reached 16.8 kV. Satisfactory BPA degradation performance was achieved in a relatively short treatment time, which proved the superiority of non-thermal plasma treatment. Aggelopoulos et al. [91] investigated the degradation of enrofloxacin (ENRO) in aqueous solution in a gas-liquid nanosecond-pulsed dielectric barrier discharge (NSP-DBD) plasma reactor. Under the optimal pulse voltage and pulse frequency, ENRO was degraded completely (100%) after 20 min, and the corresponding energy yield was 1.1 g/kWh.

3,3',4,4'-tetrachlorobiphenyl (PCB77) was selected as the target pollutant for DBD treatment in order to verify the effectiveness of non-thermal plasma in the degradation of POPs in aqueous solution [89]. Their study showed that non-thermal plasma can effectively degrade PCB77 in aqueous solution. After DBD plasma treatment for 2 min, more than 75% of PCB77 was degraded. In addition, the biotoxicity of PCB77 degradation products was also evaluated, and it was found that DBD degradation products of PCB77 are almost non-toxic, which demonstrated that non-thermal plasma is an efficient, green, and environmentally friendly treatment technology to remove POPs from the environment.

The discharge voltage applied in non-thermal plasma significantly affects the degradation/mineralization efficiency of EOPs. On the one hand, with the increase of discharge voltage, the intensity of ultraviolet radiation increases, which leads to the improvement of pollutant oxidation. On the other hand, the number of reactive species, especially  $\bullet\text{OH}$ , increases with the discharge voltage, which may lead to enhanced degradation of pollutants. However, as the discharge voltage increases excessively, the energy yield generally decreases. It is possible that the increased discharge voltage leads to increased energy waste, indicating that more electrical energy is being converted to heat [92,93]. Therefore, reasonable control of discharge voltage is the key of non-thermal plasma technology.

The pH value of aqueous solution is also one of the key factors for the degradation of EOPs by non-thermal plasma technology. It not only affects the properties of EOPs, but also affects the generation of reactive species in the non-thermal plasma system, which is probably the main reason why the results of different studies seem contradictory. The pH dependence of degradation efficiency has been extensively studied by many researchers. In general, the formation of  $\bullet\text{OH}$  is more intense under neutral or alkaline conditions. Some previous reports also support that some reactive species (e.g.,  $\text{H}_2\text{O}_2$  and  $\text{O}_3$ ) can decompose more quickly under alkaline conditions, forming  $\bullet\text{OH}$ , leading to higher efficiency of pollutant degradation [94–96]. However, in some studies, it was found that better degradation efficiency was achieved under acidic conditions. In the study of Li et al. [97], as the pH value of the solution increased from 2.0 to 10.0, the reaction rate constants of tetracycline (TC), sulfadiazine (SD) and ciprofloxacin (CIP) decreased by 40.9%, 60.0%, and 65.0%, respectively. The lower degradation efficiency under alkaline conditions can be explained by the deprotonation of pollutant molecules, which may lead to the contraction of the bond length of pollutant molecules, thus increasing the stability of molecular structure and enhancement of hydrophilicity of pollutant molecules, thus reducing the interaction with reactive species. In addition, in the relatively high pH environment, the generated  $\bullet\text{OH}$  will be quenched by  $\text{OH}^-$  [98], thus inhibiting the degradation of pollutants. Therefore, pH is not a simple parameter, and the optimal pH value for different studies may be different, and largely depends on the chemical structure and properties of pollutants.

The reaction of EOPs with different molecular structures to oxidative attacks may be different and largely depends on the substituents on the benzene ring. Generally speaking, EOPs with stable molecular structure have strong resistance to reactive species oxidation. Li et al. [97] investigated the degradation of three antibiotics with different substituents and chemical properties by non-thermal discharge plasma oxidation, namely TC, SD, and CIP. The results showed that the three antibiotics could degrade effectively, but the reaction kinetics were different. The authors speculated that the significant difference in degradation performance of the three antibiotics may be due to their different molecular structures. To verify this experimental conclusion, the authors further determined the relationship between the chemical structure of these antibiotics and their removal efficiency by using Gaussian calculations. The ionization potential (IP) of organic compounds was calculated using the following equation (Equation (1)). Compared with SD and CIP, TC had the lowest ionization potential and was therefore more easily oxidized by reactive oxygen species (ROS). Therefore, organic pollutants with different structures have different degradation effects, which was also found in the study of Kim et al. [31]. Unfortunately, they did not explain the specific reasons. Banaschik et al. [77] explained why some pharmaceutical compounds are more recalcitrant than others. Aromatic ring systems, unsaturated bonds,



and electron donating functional groups (+I/+M) increased molecular reactivity towards plasma treatment and also towards other AOPs that are relying on the generation of  $\bullet\text{OH}$ .

$$\text{IP} = 1.3124 \times (-\epsilon\text{HOMO}) + 0.514 \text{ eV} \quad (1)$$

## 2.2. Soil Remediation

At present, there is more and more research on remediation of EOPs contaminated soil by non-thermal plasma technology, and the excellent treatment effect has gradually attracted the attention of researchers. Summaries of some representative studies are presented in Table 2.

Non-thermal plasma has been proved to be effective in repairing EOPs-contaminated soil. Aggelopoulos et al. [101] studied the degradation of atrazine (ATZ) in soil by DBD discharge plasma, and the results showed that ATZ with initial concentration of 100 and 10 mg/kg could be degraded in dry soil with a degradation efficiency of 86.9% and 98.1% after plasma treatment for 60 min, respectively. Lou et al. [105] studied the remediation of chloramphenicol (CAP)-contaminated soil by DBD plasma. The results showed that the degradation efficiency of CAP was close to 81% after 20 min of plasma treatment, which demonstrated the feasibility of non-thermal plasma in removing pharmaceutical compounds from soil. Li et al. [112] used pulsed DBD plasma system to rehabilitate phenanthrene (PHE)-contaminated soil. Under the condition of 0.6 L/min air flow and 110 V voltage, the removal efficiency can reach 87.3% within 20 min, and the energy yield is 0.01 mg/kJ.

The researchers found that water content in soil is one of the most important factors affecting the removal efficiency of non-thermal plasma. A certain amount of water molecules can promote the production of  $\bullet\text{OH}$  [114]. Wang et al. [100] demonstrated that in dry soil (0% moisture), about 65.6% of glyphosate was degraded after 45 min of DBD plasma treatment, and when soil moisture increased to 10%, the proportion increased to 86.5% over the same treatment time. However, soil moisture increased further to 20%, while glyphosate degradation efficiency decreased to 76.5%. The researchers attributed this to the fact that as the water content increased, the pores of the soil became clogged with water molecules, resulting in reduced transport of reactive species through the soil, resulting in less effective degradation of pollutants. In addition, some researchers have suggested that the presence of water contributes to this by helping dissolve organic matter in soil particles, allowing the dissolved organic matter to compete with the target pollutant for reactive species [115].

Different types of power supplies used to drive various plasma reactors also have a great impact on the efficiency of soil remediation. Recently, more and more researchers have focused on the plasma driven by nanosecond pulse power supply. Nanosecond pulsed plasmas have the following advantages: (1) higher electron energy [116,117], since most of the energy in the discharge process is used to accelerate the electron energy rather than neutral gas; (2) stronger chemical activity [118], because the nanosecond pulse discharge can produce more high-energy electrons, the inelastic collision in the discharge process is more intense, and more reactive species can be produced, the chemical activity is stronger than other discharges such as alternating current (AC) and direct current (DC); (3) better uniformity and stability [119,120]. Aggelopoulos et al. [106] studied the remediation of CIP-contaminated soil by nanosecond-pulsed DBD plasma. Under the optimal conditions (pulse voltage 17.4 kV, pulse frequency 200 Hz), CIP was completely degraded in soil (~99%), and treatment time was only 3 min, with a corresponding energy efficiency of 4.6 mg/kJ, which is quite high for soil remediation. However, the plasma discharge in this study was carried out in the gas phase above the soil surface, which would lead to poor permeability of ultraviolet radiation and reactive species produced by plasma in the soil, thus affecting the treatment effect. Hatzisymeon et al. [107] designed a new type of discharge plasma reactor to alleviate this problem. In such reactors, the reactive species produced by the discharge and plasma were produced directly in the contaminated medium, rather than in the gas

phase above the contaminated medium. Under optimized conditions, the energy efficiency of the system was 21.2 mg/kJ. In addition, this system could degrade CIP almost completely over a wide range of soil thicknesses (2.4 to 9.4 mm). At the actual concentration of CIP contamination in soil (20 mg/kg), the degradation process was very rapid and complete. At high initial contaminant concentrations (200 mg/kg), considerable degradation efficiency was also achieved. Water content of up to 10% did not appear to significantly affect process efficiency, which is important for implementation under practical conditions.

**Table 2.** Overview of work done in the degradation of EOPs in soil by non-thermal plasma.

| EDCs   |                                     |  |  |       |
|--|-------------------------------------|--|--|-------|
| Target Compounds   | Non-Thermal Plasma System           | Experimental Condition   | Results  | Ref.  |
| P-nitrophenol  | Pulsed discharge plasma             | Discharge voltage: 20 kV;<br>Frequency: 100 Hz;<br>Soil mass: 2.0 g;<br>Initial concentration: 800 mg/kg   | Degradation efficiency: 78.1%<br>(10 min)  | [99]  |
| Glyphosate   | Dielectric barrier discharge plasma | Discharge voltage: 18.0 kV;<br>Air flow rate: 1.5 L/min <sup>-1</sup> ;<br>Soil mass: 5.0 g;<br>Initial concentration: 200 mg/kg;<br>Soil moisture: 10%  | Degradation efficiency: 93.9%<br>(45 min);<br>Energy yield: 0.47 g/kWh;<br>Rate constant: 0.062 min <sup>-1</sup>  | [100] |
| Atrazine   | Dielectric barrier discharge plasma | Discharge voltage: 44.8 kV;<br>Discharge power: 0.087 W;<br>Air flow rate: 1.0 L/min;<br>Frequency: 300 Hz;<br>Soil mass: 5 g;<br>Initial concentration: 100 mg/kg   | Degradation efficiency: 86.9%<br>(60 min)  | [101] |
| Pentachlorophenol  | Pulsed corona discharge plasma      | Discharge voltage: 16.0 kV<br>Frequency: 67 Hz;<br>Air flow rate: 1.0 L/min;<br>Soil mass: 5 g;<br>Initial concentration: 200 mg/kg;<br>Pollution time: 4 h  | Degradation efficiency: 85%<br>(60 min)  | [102] |
| P-nitrophenol (PNP) and pentachlorophenol (PCP) mixtures | Pulsed corona discharge plasma      | Discharge voltage: 18 kV;<br>Frequency: 50 Hz;<br>Specific energy density: 485 J/g <sub>soil</sub> ;<br>Air flow rate: 0.5 L/min;<br>Soil mass: 5 g;<br>Initial concentration: 300 mg/kg (PNP) and 300 mg/kg (PCP) | Degradation efficiency: 86.0% (PNP) and 94.1% (PCP);<br>Energy yield: 4.01 g/kWh;<br>TOC removal efficiency: 39.2% | [103] |
| Trifluralin  | Dielectric barrier discharge plasma | Discharge voltage: 26.8 kV;<br>Frequency: 100 Hz;<br>Air flow rate: 0.075 L/min;<br>Soil mass: 10.1 g;<br>Initial concentration: 200 ppm   | Degradation efficiency: 97.3%<br>(10 min);<br>Energy yield: 4.1 mg/kJ  | [104] |
| PPCPs  |                                     |  |  |       |
| Target Compounds   | Non-Thermal Plasma System           | Experimental Condition   | Results  | Ref.  |
| Chloramphenicol  | Dielectric barrier discharge plasma | Discharge voltage: 18.4 kV;<br>O <sub>2</sub> flow rate: 0.5 L/min;<br>Soil mass: 2.5 g;<br>Initial concentration: 200 mg/kg;<br>Soil moisture content: 10%  | Degradation efficiency: 81.0%<br>(20 min)  | [105] |

Table 2. Cont.

| PPCPs                            |                                     |   |   |       |
|----------------------------------|-------------------------------------|---|---|-------|
| Target Compounds                 | Non-Thermal Plasma System           | Experimental Condition  | Results   | Ref.  |
| Ciprofloxacin                    | Dielectric barrier discharge plasma | Discharge voltage: 17.4 kV;<br>Frequency: 200 Hz;<br>Air flow rate: 1.0 L/min;<br>Soil mass: 5 g;<br>Initial concentration: 200 mg/kg;<br>Soil moisture content: 5%       | Degradation efficiency: 99% (3 min);<br>Energy yield: 4.6 mg/kJ     | [106] |
| Ciprofloxacin                    | Dielectric barrier discharge plasma | Discharge voltage: 26.8 kV;<br>Frequency: 100 Hz;<br>Air flow rate: 0.075 L/min;<br>Soil mass: 6.1 g;<br>Initial concentration: 200 mg/kg;<br>Soil moisture content: 0.1% | Degradation efficiency: 95.2% (5 min);<br>Energy yield: 21.2 mg/kJ  | [107] |
| POPs                             |                                     |   |   |       |
| Target Compounds                 | Non-Thermal Plasma System           | Experimental Condition  | Results   | Ref.  |
| Pyrene                           | Dielectric barrier discharge plasma | Discharge voltage: 36.2 kV;<br>Electrode gap: 14 mm;<br>Initial concentration: 100 mg/kg  | Degradation efficiency: 61.6% (60 min)                              | [108] |
| Fluorene                         | Corona discharge plasma             | Discharge voltage: 30 kV;<br>Frequency: 50 Hz;<br>Electrode gap: 20 mm;<br>Initial concentration: 200 mg/kg   | Degradation efficiency: 78.7% (60 min)                              | [109] |
| Naphthalene                      | Dielectric barrier discharge plasma | Discharge voltage: 40 kV;<br>Air flow rate: 0.85 L/min;<br>Moisture contents: 4%;<br>Soil depth: 1 mm;<br>Initial concentration: 100 mg/kg                                | Degradation efficiency: 96.32% (30 min)                             | [110] |
| Phenanthrene                     |                                     |   | Degradation efficiency: 89.08% (30 min)                             |       |
| Pyrene                           |                                     |   | Degradation efficiency: 88.59% (30 min)                             |       |
| Pyrene                           | Dielectric barrier discharge plasma | Discharge voltage: 35.8 kV;<br>Frequency: 9 kHz;<br>Air flow rate: 0.85 L/min;<br>Initial concentration: 10 mg/kg   | Degradation efficiency: 85.09% (30 min);<br>Energy yield: 0.8 µg/kJ | [111] |
| Phenanthrene                     | Dielectric barrier discharge plasma | Discharge voltage: 110 V;<br>Frequency: 150 Hz;<br>Air flow rate: 0.6 L/min;<br>Soil mass: 5 g;<br>Initial concentration: 200 mg/kg                                       | Degradation efficiency: 87.3% (20 min);<br>Energy yield: 0.01 mg/kJ | [112] |
| Polychlorinated biphenyls        | Dielectric barrier discharge plasma | Discharge power: 21 W;<br>Gas flow rate: 120 mL/min;<br>Initial concentration: $1.78 \times 10^4$ µg/kg   | Degradation efficiency: 84.6% (90 min)                              | [113] |
| Polycyclic aromatic hydrocarbons | Pulsed corona discharge plasma      | Discharge voltage: 18 kV;<br>Frequency: 70 Hz;<br>Air flow rate: 0.8 L/min;<br>Initial concentration: 100 mg/kg   | Degradation efficiency: 70% (40 min)                                | [36]  |

### 2.3. Comparison with Other AOPs

Comparisons between non-thermal plasma and other AOPs are difficult because experimental conditions (such as molecular structure, initial concentration, treatment

volume, etc.) vary greatly and these parameters significantly affect the degradation process. In order to find a more accurate evaluation of degradation efficiency and energy yield, Hama Aziz et al. [74,121] focused on the degradation of 2,4-dichlorophenoxyacetic acid (2,4-D), 2,4-dichlorophenol (2,4-DCP), diclofenac (DCF), and ibuprofen (IBP) by several AOPs: ozonation, photocatalysis, and non-thermal plasma. The common reactor design of all experiments can directly compare the degradation efficiency and energy yield obtained by different methods. The specific comparison results are shown in Table 3. Comparing these AOPs from the perspective of degradation efficiency and energy yield, it is found that there is an obvious gap in the degradation of pollutants with different molecular structures, which indicates that different AOPs will be affected by the molecular structure.

**Table 3.** Comparison of EOPs degradation by non-thermal plasma and other AOPs.

| Target Pollutant | Technology         | Initial Concentration (mg/L) | Solution Volume (mL) | Treatment Time (min) | Degradation Efficiency | Energy Yield G <sub>50</sub> (g/kWh) | References |
|------------------|--------------------|------------------------------|----------------------|----------------------|------------------------|--------------------------------------|------------|
| 2,4-D            | Ozonation          | 100                          | 500                  | 20                   | ~100%                  | 6.60                                 | [121]      |
|                  | Photocatalysis     |                              |                      | 90                   | 67%                    | 0.92                                 |            |
|                  | Non-thermal plasma |                              |                      | 15                   | ~100%                  | 8.80                                 |            |
| 2,4-DCP          | Ozonation          | 100                          | 500                  | 10                   | ~100%                  | 18.09                                |            |
|                  | Photocatalysis     |                              |                      | 90                   | 73%                    | 0.35                                 |            |
|                  | Non-thermal plasma |                              |                      | 15                   | ~100%                  | 4.64                                 |            |
| DCF              | Ozonation          | 50                           | 500                  | 4                    | ~100%                  | 28.00                                | [74]       |
|                  | Photocatalysis     |                              |                      | 90                   | ~80%                   | ~0.50                                |            |
|                  | Non-thermal plasma |                              |                      | 20                   | ~100%                  | 5.10                                 |            |
| IBP              | Ozonation          | 50                           | 500                  | 25                   | ~100%                  | 2.50                                 |            |
|                  | Photocatalysis     |                              |                      | 90                   | ~35%                   | ~0.25                                |            |
|                  | Non-thermal plasma |                              |                      | 15                   | ~100%                  | 2.15                                 |            |

Compared with photocatalysis, ozonation, and non-thermal plasma have the advantages of fast degradation rate, high degradation efficiency, and high energy yield. It can also be seen from Table 3 that ozonation and non-thermal plasma show similar performance. Taking 2,4-D as an example, the energy yield of non-thermal plasma is 8.8 g/kWh, while the energy yield of ozonation for the removal of 2,4-D is 6.6 g/kWh. It is worth noting that the mineralization efficiency of pollutants by ozonation is relatively low, and very good mineralization can be obtained by non-thermal plasma. Li et al. [122] compared the degradation of IBP by different AOPs. Except that the energy yield of photo-Fenton is slightly higher than that of water film DBD plasma, the energy yield of other AOPs is relatively low. However, photo-Fenton takes a longer time and the removal efficiency is not very high.

### 3. Mechanism of Emerging Organic Pollutants Degradation by Non-Thermal Plasma

#### 3.1. Reactive Species in Non-Thermal Plasma Discharges

The ability of non-thermal plasma to produce highly reactive species in situ is well known. Their formation is mainly triggered by the collision of high-energy electrons produced in the discharge with gas atoms or molecules. Once the discharge process has occurred, reactive species can also be produced by radical recombination reactions or de-excitation of metastable substances [96]. The most abundant primary and secondary species formed in liquid or gas-liquid environments are hydroxyl radical ( $\bullet\text{OH}$ ), ozone ( $\text{O}_3$ ), and hydrogen peroxide ( $\text{H}_2\text{O}_2$ ), which are associated with the degradation of target pollutants. However, many other ROS and RNS are produced in plasma, and can also contribute to the decomposition of pollutants, such as singlet oxygen ( $^1\text{O}_2$ ), atomic oxygen ( $\text{O}$ ), superoxide anion radical ( $\bullet\text{O}_2^-$ ), peroxide hydroxyl radical ( $\text{HO}_2\bullet$ ), nitrite ( $\text{NO}_2^-$ ), nitrate ( $\text{NO}_3^-$ ), peroxyxynitrite ( $\text{ONOO}^-$ ), etc. The redox potentials of common oxidants are shown in Figure 2. These reactive species react with pollutants in water or soil, or high-energy electrons in an electric field react directly with pollutants, degrading them into small intermediates and further splitting them into carbon dioxide and water molecules. In

addition to oxidizing species, reductive species in discharge plasma may also contribute to the degradation of pollutants in water, such as aqueous electron ( $E^0 = -2.77$  V) and  $H\bullet$  radicals ( $E^0 = -2.30$  V). Furthermore, some physical effects, such as ultraviolet radiation, heat, and shock wave, are often accompanied in the plasma discharge process. In conclusion, the degradation of organic compounds by discharge plasma depends mainly on the reactive species, while other physical effects are beneficial to the degradation process.

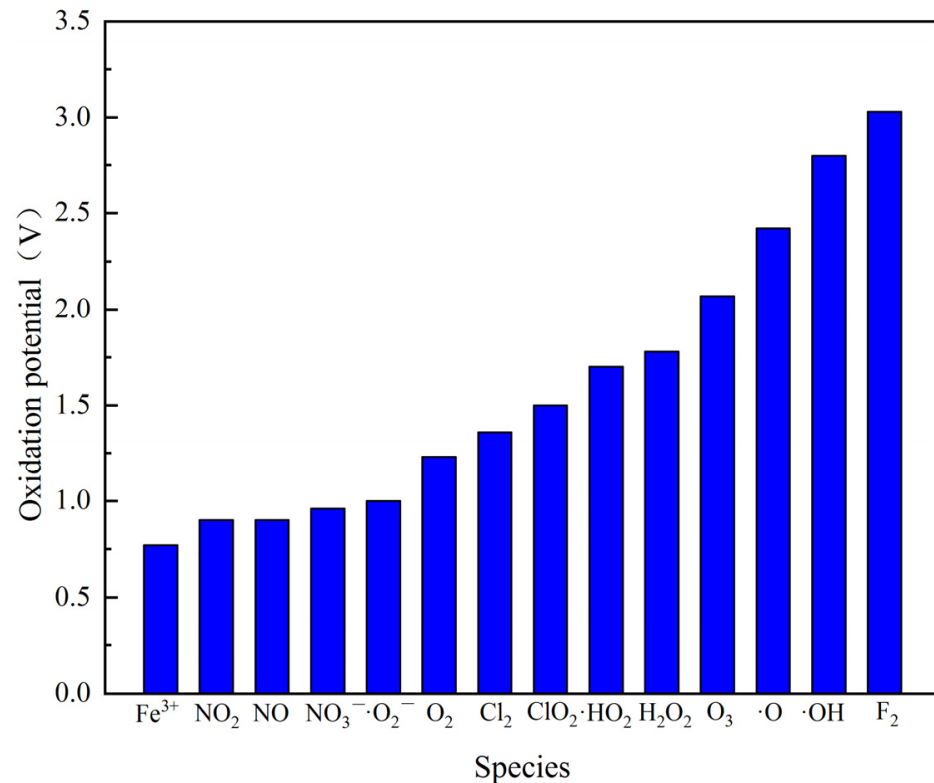
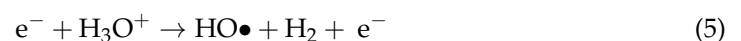


**Figure 2.** Comparison of oxidation potential of reactive species by non-thermal plasma.

$\bullet OH$  is the second most reactive substance after fluorine atom, and they attack most organic pollutant molecules with a rate constant of  $10^6$ – $10^9$   $M^{-1} s^{-1}$ , which is  $10^6$ – $10^{12}$  times faster than ozone [123,124]. The production of  $\bullet OH$  in water or plasma in contact with water was discussed in detail [125]. Bruggeman et al. found that the production of  $\bullet OH$  depends largely on plasma parameters, such as gas temperature ( $T_g$ ), electron temperature ( $T_e$ ), ionization degree, electron and ion density, and gas composition. The results showed that  $\bullet OH$  formed by electron dissociation (Equation (2)) and dissociation attachment (Equation (3)) of water molecules are dominant in plasma with  $T_e$  higher than 2 eV. However, when  $T_e$  is between 1 and 2 eV, electron-ion dissociation recombination (Equations (4) and (5)) and ion-ion dissociation recombination (Equations (6) and (7)) also play an important role in the mass production of  $\bullet OH$ . Even at high enough ionization degree, it is also the main formation pathway of  $\bullet OH$ .



In the case of air or oxygen as the feed gas, O<sub>3</sub> is formed by non-thermal plasma, and the process has been well documented [126]. The electrons generated in the discharge excite and dissociate diatomic oxygen (Equation (8)), and the resulting atomic oxygen reacts with another oxygen molecule in the presence of a third object (M: M is a third collision partner: O<sub>2</sub>, O<sub>3</sub>, O) to form ozone (Equation (9)).



It is generally believed that H<sub>2</sub>O<sub>2</sub> is mainly formed by the dimerization of •OH in discharge in contact with water (Equation (10)):



H<sub>2</sub>O<sub>2</sub> is a relatively stable oxidant and can accumulate in the liquid phase during plasma discharge. Locke and Shih [127] summarized the literature on the formation of H<sub>2</sub>O<sub>2</sub> in water using various discharge techniques and experimental conditions. The results showed that the efficiency of H<sub>2</sub>O<sub>2</sub> production depends largely on the experimental device, and the maximum energy yield is 80 g/kWh. In addition to the direct generation of •OH in the plasma, additional •OH may be generated by the interaction of dissolved O<sub>3</sub> with H<sub>2</sub>O<sub>2</sub> (Equation (11)).



Formation of more •OH is particularly beneficial for degradation because •OH is a powerful non-selective oxidant that reacts with most organic compounds, including short-chain carboxylic acids, and complex intermediates produced during degradation of organic molecules. Thus, increased concentrations of •OH can ensure further degradation/mineralization of organic pollutants.

In the study of plasma discharge technology using air/N<sub>2</sub> as raw gas, in addition to ROS, RNS are also formed, such as nitric oxide (NO), nitrogen dioxide (NO<sub>2</sub>), nitrite (NO<sub>2</sub><sup>-</sup>), nitrate (NO<sub>3</sub><sup>-</sup>), and peroxyxynitrite (ONOO<sup>-</sup>) [95]. Even though N<sub>2</sub> is a very stable molecule with high bonding energy, high-energy electrons generated during plasma discharge can dissociate the molecule from atomic nitrogen (Equation (12)). Nitrogen oxides are then rapidly formed by the interaction of atomic nitrogen with diatomic or triatomic oxygen (Equations (13) and (14)). The exchange between the two nitrogen oxides can be achieved by the interaction of nitric oxide with ozone and the photodissociation of nitrogen dioxide by ultraviolet radiation produced in the plasma (Equations (15) and (16)). Further dissolution and oxidation of nitrogen oxides in aqueous media lead to the formation of NO<sub>2</sub><sup>-</sup>, NO<sub>3</sub><sup>-</sup>, and ONOO<sup>-</sup>.



### 3.2. Degradation Pathways of Emerging Organic Pollutants

Different degradation efficiencies and rates have been recorded using non-thermal plasma techniques for different classes of EOPs. This phenomenon is mainly due to the different chemical structure of EOPs. Different kinds of organic compounds require different amounts of energy to break bonds. Therefore, the complexity of degradation pathway is also a key factor in the final degradation results. During non-thermal plasma treatment, in addition to the residue of the target pollutant, some intermediates also



exist in the water/soil, which will compete with the target pollutant for reactive species, resulting in poor degradation. However, little is known about the differences in degradation mechanisms and kinetics. Therefore, the degradation pathways of some different types of EOPs are summarized below.

### 3.2.1. Selected EDCs: Bisphenol A

Based on most relevant research, the results suggested that  $\bullet\text{OH}$ ,  $\text{O}_3$  and  $\bullet\text{NO}_2$  play an important role in the degradation of BPA and most intermediates. Generally, there are two main pathways for the degradation of BPA in non-thermal plasma [56–59], as shown in Figure 3. On the one hand,  $\bullet\text{OH}$  reacts with phenolic hydroxyl groups in BPA to form TP1 through hydrogen abstraction. The C atom on the ortho position of the hydroxyl group of TP1 undergoes hydroxylation and a recombination reaction under the attack of  $\bullet\text{OH}$  and  $\bullet\text{NO}_2$  to generate TP2 and TP3. Then, TP4 and TP5 are generated by tautomerization of the keto and enol forms. On the other hand, the C atom between the two benzene rings is cleaved under the oxidation of  $\bullet\text{OH}$  and  $\text{O}_3$  to generate TP6 and TP7. In addition, the above intermediate products can be further oxidized and ring-opened to generate a series of small molecular organic compounds, and finally mineralized into  $\text{CO}_2$  and  $\text{H}_2\text{O}$ .

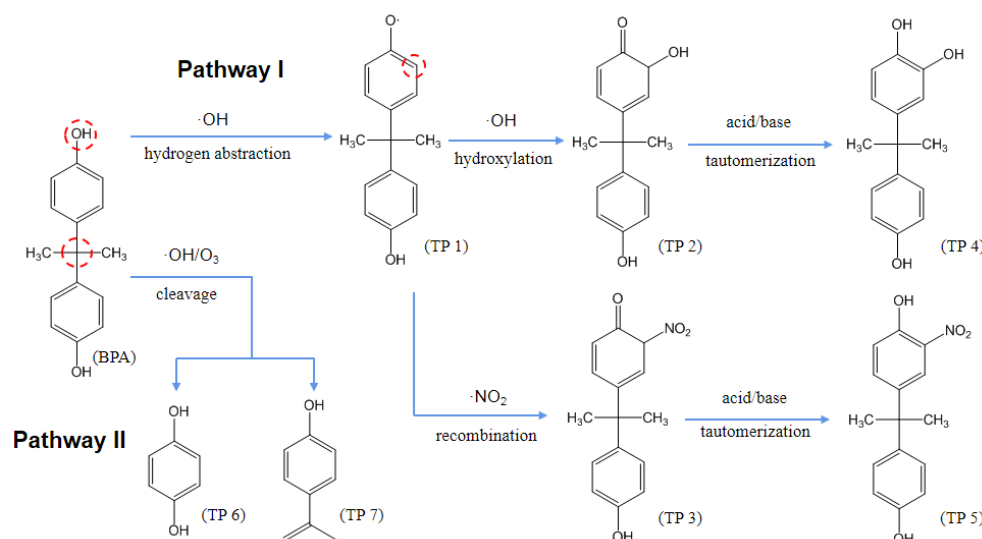


**Figure 3.** The proposed BPA degradation pathway.

### 3.2.2. Selected PPCPs: Ibuprofen

Based on density functional theory (DFT), the spatial configuration of organic molecules and electron cloud density distribution can be obtained by molecular orbital calculation, which is helpful to predict the degradation behavior of organic pollutants. Generally, there are three common pathways for IBP to undergo degradation by non-thermal plasma, as shown in Figure 4. First,  $\bullet\text{OH}$  can cause IBP to lose its carboxyl structure to generate the product TP1. TP1 is further deprotonated to form an intermediate product TP2 under the oxidation of  $\bullet\text{OH}$ ,  $\text{O}_3$  and other reactive species. Then, TP3 and TP4 are generated through hydroxylation and demethylation reactions. Secondly, the 10C in molecular structure of IBP is prone to hydroxylation to form TP5. Next, TP5 is deprotonated to form the product TP6, followed by demethylation and decarboxylation under the action of reactive species to generate TP7 and TP8 in turn. Li et al. [122] proposed the possible degradation pathway of IBP in DBD plasma based on DFT analysis. DFT was used to describe the molecular properties of IBP, which can reveal the potential of IBP in specific degradation reactions, as well as the optimal location of electrophilic or nucleophilic reactions in the molecule. The results showed that the 2 and 5 C positions of IBP are vulnerable to attacks by electrophiles and nucleophiles. Therefore, the third degradation pathway of IBP begins with the attack of the 2 or 5 C atom by the  $\bullet\text{OH}$ . TP9 and P10 are generated by the substitution of  $\bullet\text{OH}$ ,

and subsequent hydroxylation, demethylation, and deprotonation reactions may also occur to generate a series of intermediate products. Finally, the benzene ring undergoes a ring-opening process to form formic, acetic, and oxalic acids. These organic acid molecules continued to mineralize into CO<sub>2</sub> and H<sub>2</sub>O.

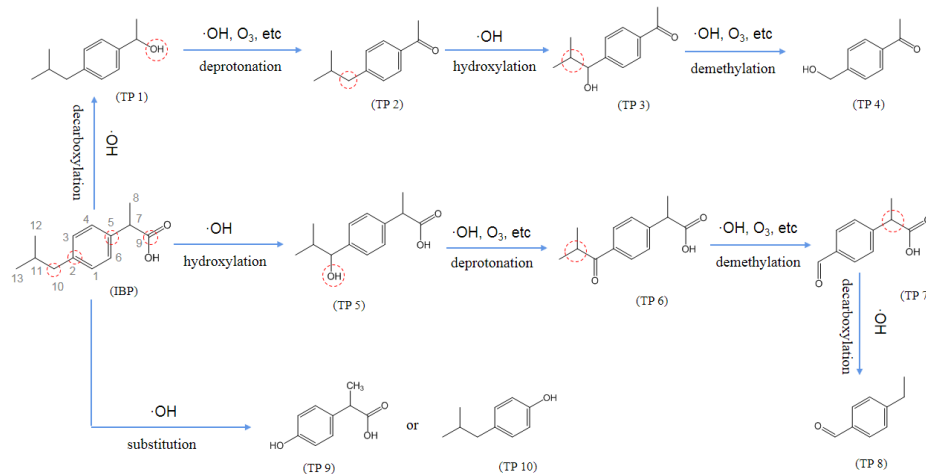


Figure 4. The proposed IBP degradation pathway.

### 3.2.3. Selected POPs: PCB77

The dechlorination of PCBs has always been the most important step in their degradation process. Huang et al. [89] applied DBD non-thermal plasma for the degradation of PCB77, and its degradation process and common reaction sites are shown in Figure 5. Firstly, •OH causes the dechlorination reaction of PCB77 and generates a series of the dechlorination product TP1. Due to the different reactivity of different sites on the benzene ring, the selectivity of the dechlorination reaction usually depends on the position of the chlorine atom, following the order of para > meta > ortho [128]. Secondly, •OH can lead to a benzene cycloaddition reaction, forming multiple C-OH when all C-Cl break. Since the O atom in the phenolic hydroxyl group can undergo p-π conjugation with the benzene ring, the p electron cloud is transferred to the benzene ring, which increases the electron cloud density on the benzene ring and is easy to attack by electrophiles [129,130]. Numerous sites on the benzene ring are attacked by various reactive species in the plasma, and then partially cleaved to form the intermediate product TP2. The aromatic ring structure in TP2 may be attacked to form unstable products through electrophilic addition. Finally, the above intermediate products are degraded into smaller organic molecules, CO<sub>2</sub> or inorganic salts.

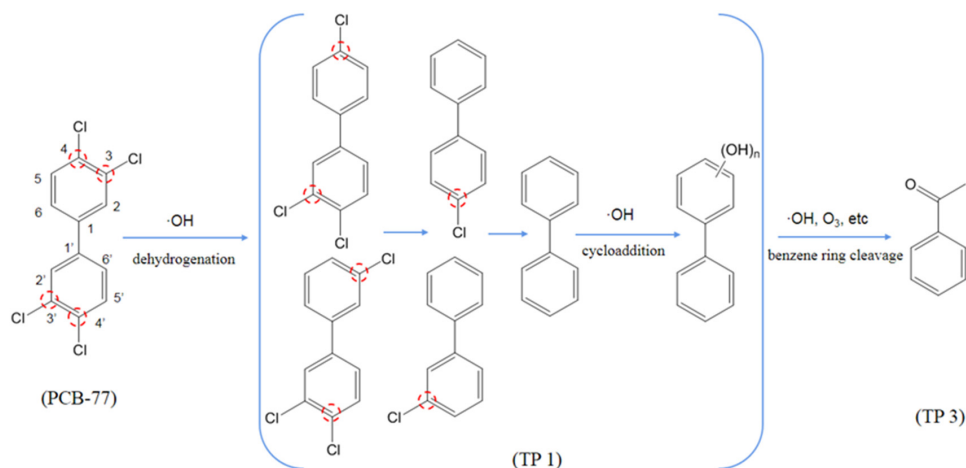


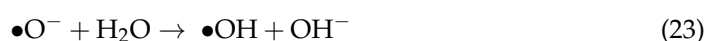
Figure 5. The proposed PCB77 degradation pathway.

#### 4. Non-Thermal Plasma and Other Technologies Cooperate to Degrade Emerging Organic Pollutants in Environment

Because most single methods have some defects, it has been fully proved in various research fields to make up for the shortcomings of a single system by using it in combination with other methods [131,132]. Non-thermal plasma is a kind of AOPs which integrates many factors, such as reactive species, high-energy electrons, ultraviolet radiation, and so on, which shows good characteristics in the process of dealing with EOPs. However, non-thermal plasma also has some disadvantages, such as low utilization efficiency of active components and ultraviolet radiation, low energy utilization efficiency, and so on [72,133]. In view of these limiting factors, the synergistic plasma technology of oxidants and catalysts will become one of development trends in the future. Another barrier to plasma is the low mass transfer efficiency of the resulting reactive species from the plasma to the phase where pollutants are present. Therefore, when designing a plasma reactor, it is necessary to consider not only the generation of these reactive species, but also their efficient transfer to the target pollutants. Recently, microbubbles (MBs) have been considered as an effective method to improve the efficiency of plasma reactors. However, only few studies have been carried out, and its mechanism is still unclear. Therefore, it is necessary to study the effects of MBs on improving gas-liquid mass transfer in water treatment and the development of other means to improve the mass transfer efficiency of reactive species from plasma to medium is also the focus of plasma research in the future.

##### 4.1. Oxidant

In recent years, the AOPs based on sulfate radical ( $\bullet\text{SO}_4^-$ ) has attracted much attention because of its high oxidation activity and good adaptability to various EOPs. The redox potential of  $\bullet\text{SO}_4^-$  (2.5–3.1 V) is higher than that of  $\bullet\text{OH}$  (1.9–2.7 V), and the half-life of  $\bullet\text{SO}_4^-$  (30–40  $\mu\text{s}$ ) is much longer than that of  $\bullet\text{OH}$  ( $10^{-3}$   $\mu\text{s}$ ), which is beneficial to improve the degradation efficiency of pollutants [134]. Ultraviolet radiation, local high temperatures, and hydrated electrons produced by non-thermal plasma can activate persulfate (PS) to form  $\bullet\text{SO}_4^-$ , which helps improve the energy efficiency of the plasma system (Equations (17) and (18)) [135,136]. Tang et al. [65] studied the degradation of TC in water by gas surface discharge plasma-activated PS. With the increase of the PS dosage, the removal efficiency of TC in DBD plasma was also significantly improved. The calculated synergistic factor was 1.856, indicating that the addition of PS has an obvious synergistic effect. Wu et al. [133] found that the addition of peroxymonosulfate (PMS) into the DBD plasma can increase the degradation efficiency of benzotriazole (BTA) by 47%. In addition, energy production increased by 84%. The improvement of BTA degradation efficiency may be attributed to the activation of PMS by plasma, which increases the formation of reactive species and  $\bullet\text{SO}_4^-$ . In addition, some studies have shown that the introduction of PMS can realize the secondary utilization of  $\text{O}_3$  (Equations (19)–(23)) [135].



In addition, oxidants, such as percarbonate (SPC), ferrate, and  $\text{H}_2\text{O}_2$ , were also used in non-thermal plasma. Tang et al. [137] explored the synergistic effect of SPC and plasma, and the results showed that the addition of SPC was beneficial to the production of  $\text{H}_2\text{O}_2$

and the decomposition of  $O_3$ . When SPC was 52.0 mol/L and voltage was 4.8 kV, the removal efficiency of TC could reach 94.3% at 20 mg/L. Xu et al. [138] found that low concentration (0.1–1.0 mmol/L) of  $H_2O_2$  could promote the degradation of norfloxacin (NOR) by plasma, while high concentration (1.0–2.0 mmol/L) of  $H_2O_2$  could inhibit the degradation of NOR. Sang et al. [139] compared the effect of PMS, SPC, and ferrate on the degradation of Orange G (OG) by DBD plasma, and found that the degradation efficiency of OG by ferrate plasma was the best. The possible mechanism of degradation of EOPs by non-thermal plasma combined with different oxidants is shown in Figure 6.

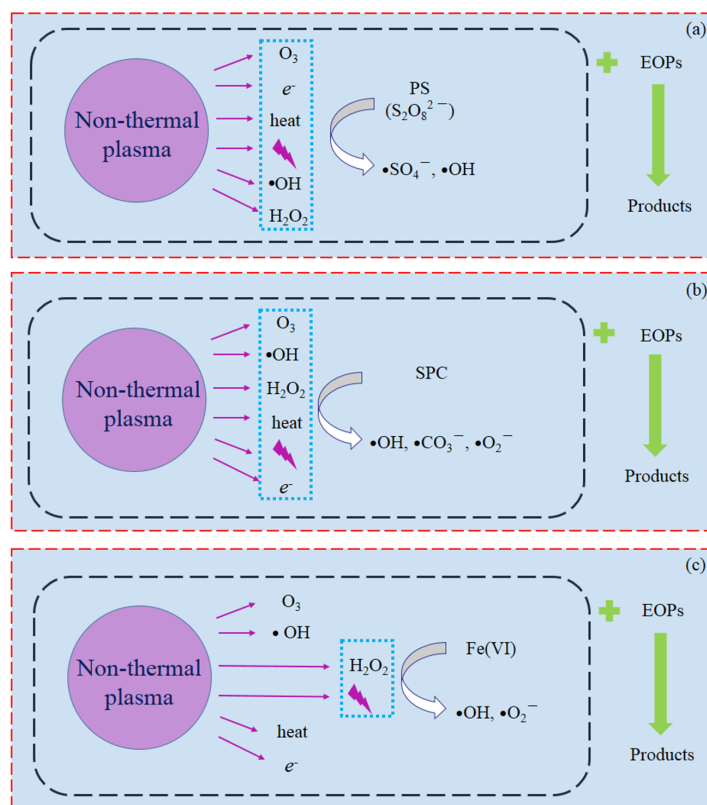
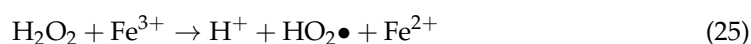
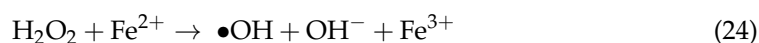


**Figure 6.** Possible degradation mechanisms of EOPs combined with different oxidants: (a) PS, (b) SPC, (c) Fe (VI).

## 4.2. Catalyst

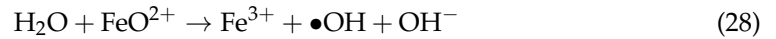
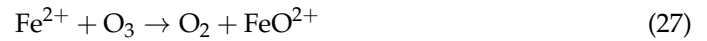
### 4.2.1. Homogeneous Catalyst

$Fe^{2+}$  is the most commonly used homogeneous catalyst in combination with non-thermal plasma. The addition of  $Fe^{2+}$  can form a Fenton system with the non-thermal plasma and produce more  $\bullet OH$  to degrade EOPs (Equations (24) and (25)) [140,141]. Hao et al. [142] introduced iron ion ( $Fe^{2+}/Fe^{3+}$ ) into the pulsed discharge plasma system. The experimental results showed that the addition of iron ion ( $Fe^{2+}/Fe^{3+}$ ) could greatly improve the removal efficiency of 4-chlorophenol. At the same time, they found that the promoting effect of  $Fe^{2+}$  was greater than that of  $Fe^{3+}$ . Xu et al. [138] found that a low concentration of  $Fe^{2+}$  can promote the degradation of NOR by DBD plasma, while a high concentration can inhibit the degradation of NOR, which may be due to the reaction of excessive  $Fe^{2+}$  with  $\bullet OH$  to form  $Fe^{3+}$  and  $OH^-$  (Equation (26)). At the same time, the  $Fe^{3+}$  can also react with  $H_2O_2$  in aqueous solution (Equation (25)), thus reducing the concentration of  $H_2O_2$ .





In addition, the oxidizability of  $\text{O}_3$  produced by non-thermal plasma is lower than that of  $\bullet\text{OH}$ , while the introduction of  $\text{Fe}^{2+}$  can react with  $\text{O}_3$  to form  $\bullet\text{OH}$  (Equations (27) and (28)), thus improving the  $\bullet\text{OH}$  content and energy efficiency of the non-thermal plasma.



#### 4.2.2. Heterogeneous Catalyst

Non-thermal plasma co-heterogeneous catalytic oxidation technology refers to the addition of solid catalyst (generally used in powder form) in the discharge region of the plasma. Catalysts react with ultraviolet radiation or reactive species such as ozone and hydrogen peroxide generated in plasma discharge process, and then trigger a series of chain reactions to promote the generation of active free radicals and degradation of organic matter. Furthermore, the combined adsorption and catalytic action of catalysts with a large specific surface area can contribute to the removal of pollutants. Compared with other advanced oxidation technologies, plasma discharge has a variety of physical and chemical effects, such as high electric field, shock wave, etc., which can clean the surface of accelerators and contribute to the regeneration of catalysts [143]. At present, the solid catalysts used for plasma catalytic oxidation mainly include carbon catalysts represented by activated carbon, photocatalysts represented by  $\text{TiO}_2$ , other metal catalysts, metal or metal oxide catalysts supported on supports, etc. The possible mechanism of degradation of EOPs by non-thermal plasma combined with heterogeneous catalyst is shown in Figure 7.

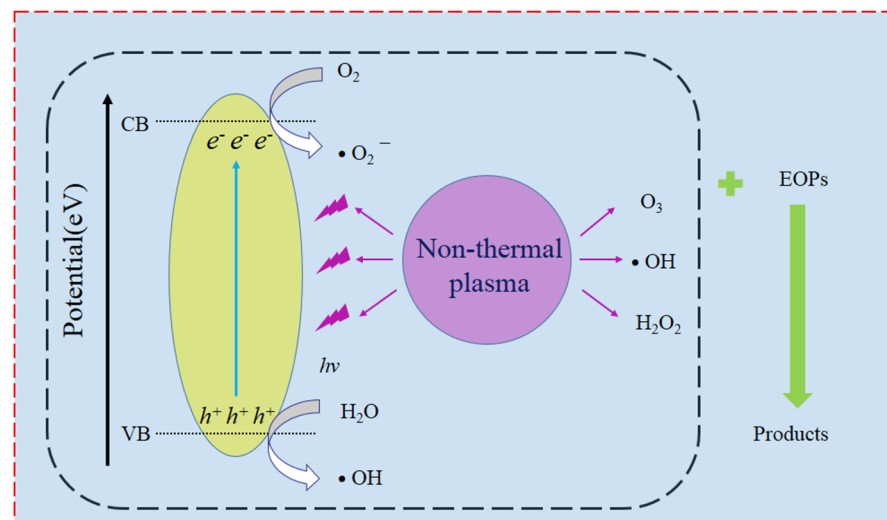
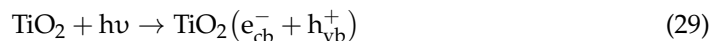


**Figure 7.** Possible degradation mechanisms of EOPs combined with heterogeneous catalyst.

Different from the homogeneous catalyst, the heterogeneous catalyst is easy to recover and separate; so, there are many studies on the coupling of the heterogeneous catalyst and plasma to degrade EOPs. Guo et al. [69] coupled pulsed discharge plasma (PDP) with  $\text{Fe}_3\text{O}_4$  to promote the degradation of CAP. In PDP system,  $\text{Fe}_3\text{O}_4$  not only catalyzed  $\text{H}_2\text{O}_2$  to form a Fenton reaction, but also catalyzed  $\text{O}_3$ , which promotes the formation of  $\bullet\text{OH}$ . When the addition amount of  $\text{Fe}_3\text{O}_4$  is 0.26 g/L, under the conditions of higher peak voltage, lower initial solution concentration, and lower initial pH value, CAP is beneficial to decomposition and has the best catalytic performance. Cheng et al. [144] used  $\alpha\text{-MnO}_2$ ,  $\beta\text{-MnO}_2$ , and  $\gamma\text{-MnO}_2$  to degrade CIP wastewater by DBD plasma-catalytic combined process. The results showed that the combination of DBD plasma and  $\alpha\text{-MnO}_2$  has the highest degradation efficiency of CIP, and the degradation efficiency could reach 93.1%, which was 10.8% and 18.1% higher than that of  $\beta\text{-MnO}_2$  and  $\gamma\text{-MnO}_2$  catalyst in the plasma

catalytic system, respectively. The photocatalyst TiO<sub>2</sub> can enhance the degradation of EOPs in the plasma system by utilizing the ultraviolet radiation produced by the plasma (Equations (29) and (30)) [145]. Lee et al. [83] found that the addition of TiO<sub>2</sub> increased the decomposition rate of DMP, but the excess dosage of TiO<sub>2</sub> resulted in ultraviolet radiation blocking and decreased the decomposition rate of DMP. Jogi et al. [146] found that the addition of TiO<sub>2</sub> can increase the amount of O<sub>3</sub> produced by the DBD plasma, which may be one of the reasons for improving the efficiency of pollutant degradation.



A single metal oxide photocatalyst has a high recombination rate for electron-hole pairs generated by light energy and is only sensitive to ultraviolet light, while catalysts such as Fe<sub>3</sub>O<sub>4</sub> can use H<sub>2</sub>O<sub>2</sub> and O<sub>3</sub> but cannot use ultraviolet light [64,71]. Therefore, it is an ideal choice to prepare composite catalysts from metal oxides and other catalysts [147]. In order to make full use of the ultraviolet light generated by the plasma, Fe<sub>3</sub>O<sub>4</sub> was supported on reduced graphene oxide (rGO) [71]. Compared with using Fe<sub>3</sub>O<sub>4</sub> alone, rGO-Fe<sub>3</sub>O<sub>4</sub> further improved the degradation efficiency and kinetic constant of ofloxacin in the discharge plasma system. After 60 min of treatment, the degradation efficiency and kinetic constant reached 99.9% and 0.108 min<sup>-1</sup>, respectively.

In addition, composite catalysts composed of metal oxides and metal oxides, metal oxides, and metal elements are also used in non-thermal plasma. Ansari et al. [68] combined a ZnO/α-Fe<sub>2</sub>O<sub>3</sub> composite catalyst with DBD plasma to degrade antibiotic amoxicillin (AMX). The results showed that the ZnO/α-Fe<sub>2</sub>O<sub>3</sub> composite catalyst increased the degradation efficiency of AMX from 75.0% (sole DBD plasma) to 99.3% under optimal conditions. Wang et al. [148] found that compared with the plasma process, the combination of plasma and Mn/γ-Al<sub>2</sub>O<sub>3</sub> catalyst significantly improved the degradation efficiency of tetracycline hydrochloride. Under the discharge power of 1.3 W, the degradation efficiency of tetracycline hydrochloride could reach 99.3%, while the degradation efficiency of the plasma treatment was only 69.7%.

At present, plasma-catalytic systems are mainly focused on water remediation, but there are few reports about soil remediation. However, it has been demonstrated that plasma-catalytic systems improve the efficiency of plasma systems in soil remediation. Wang et al. [99,149] investigated the degradation of p-nitrophenol (PNP) in soil using a pulsed discharge plasma-TiO<sub>2</sub> catalytic system. Compared with the single plasma system, the system showed higher degradation performance of PNP. Increased TiO<sub>2</sub> content promoted PNP degradation to a certain extent, while further increased TiO<sub>2</sub> content had negative effects. At higher TiO<sub>2</sub> content, particles aggregation may reduce the interface area between contaminants and catalyst surface sites, thereby reducing the number of active sites on the catalyst surface and resulting in reduced PNP degradation [150].

In conclusion, the combination of plasma discharge and catalyst reveals the catalytic promoting effect on pollutant removal and improves the efficiency of non-thermal plasma.

#### 4.3. Microbubbles

MBs generally refer to bubbles with equivalent diameters less than 50 μm. Compared with millimeter-sized bubbles, MBs have some special properties that can enhance the discharge effect. Firstly, the gas-liquid mass transfer ability of MBs is strong. Unlike millimeter-sized bubbles, MBs will not rise rapidly from the water to the liquid surface and break. The rising speed of MBs in water is slower than that of millimeter-sized bubbles, and the residence time in water is longer, which greatly prolongs the gas-liquid contact time [151,152]. Figure 8 shows the characteristics of millimeter-sized bubbles and micron-sized bubbles in water. Secondly, MBs can stimulate the generation of free radicals in the process of fragmentation. Adiabatic compression occurs during bubble contraction, which generates local high temperature and high pressure around the bubble. Such conditions



stimulate the decomposition of water molecules around the bubble into free radicals [153]. Takahashi et al. [152] demonstrated free-radical generation from the collapse of MBs in the absence of a harsh dynamic stimulus. Electron spin-resonance spectroscopy confirmed free-radical generation by the collapsing MBs. The increase of the surface charges ( $\zeta$  potentials) of the MBs, which were measured during their collapse, supported the hypothesis that the significant increase in ion concentration around the shrinking gas-water interface provided the mechanism for radical generation.

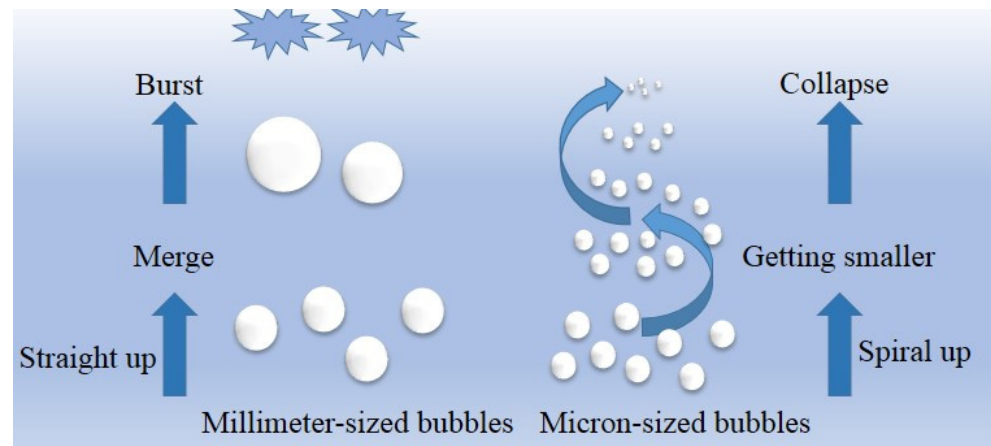


**Figure 8.** Comparison of millimeter-sized bubbles and micron-sized bubbles in water.

Studies showed that compared with plasma treatment alone, the presence of MBs can significantly improve the treatment efficiency, and preliminary studies speculate that the presence of MBs can improve gas-liquid mass transfer in plasma water treatment [154,155]. MBs were introduced with different carrier gases (air,  $N_2$  and Ar) in the needle-plate pulsed discharge reactor to enhance the interface reaction [156]. Due to the surface  $\zeta$ -potential, MBs can effectively enrich pollutants, and the large specific surface area also leads to a high gas-liquid interface area, which enhances the plasma reaction with pollutants. At the same time, these unique physical properties can also promote the mass transfer from gas to liquid in the system. Wang et al. [157] evaluated the degradation of ATZ in aqueous solution by DBD/MBs/PS system in order to develop a more efficient and environmentally friendly PS activation method. The observed ATZ removal efficiency (DBD/MBs/PS > DBD/PS > MBs/PS) confirmed the synergistic effect of DBD/MBs/PS. Based on the ATZ removal efficiencies of 64% and 56% in DBD/MBs/PS and DBD/PS systems, the mass transfer contribution rate was calculated as 13% in DBD/MBs/PS system. The synergies of DBD/MB/PMS systems are largely due to the interaction between DBD, MBs, and PMS. DBD plasma produces a large number of reactive species when gas molecules dissociate and form high-energy electrons. By combining DBD plasma and MBs, the plasma can be ignited inside the MBs, where an electron avalanche breakdown occurs and continues until the MBs crashes.

## 5. Practical Implications of This Study

Among a large number of research works in the past decade, non-thermal plasma technology has been proved to be a promising environmental remediation technology. However, there are still some challenges to be solved and breakthroughs to be made.

- (1) One of the most serious challenges of non-thermal plasma technology is how to improve the energy yield of the treatment system and reduce the operation cost. According to the summary of existing research, the energy yields of different research results vary greatly, covering several orders of magnitude. In addition to the different molecular structures of pollutants, the design and experimental conditions of a non-thermal plasma reactor also have a great influence. Due to the particularity of in situ generation of reactive species by non-thermal plasma, the main improvement of

reactor design mainly lies in how to maximize the generation of reactive species and effectively transfer them to the medium where pollutants exist.

- (2) In addition, non-thermal plasma technology is still in the laboratory research stage, and the volume of the reactor is too small to be put into practical application. Therefore, how to expand the scale of the reactor is a major challenge for future research.
- (3) Another key research challenge is that the current research mainly focuses on the degradation efficiency of pollutants and lacks the toxicity test of water and soil environment after non-thermal plasma treatment, which is very important for the practical application of non-thermal plasma technology in the future. Although it is generally shown that non-thermal plasma can reduce the concentration of pollutants, the toxicity of the degradation products and the ultimate impact of reactive species produced by non-thermal plasma that may persist are not clear. This is a problem that needs to be analyzed in more detail in the future.

Some suggestions for future development direction are also put forward.

- (1) At present, most research focuses on artificially polluted water and soil, and research on actually polluted water and soil is limited. Therefore, more attention should be paid to the actually polluted water or soil, which may promote the practical application of non-thermal plasma in the future.
- (2) It is well known that the traditional sewage treatment process of sewage treatment plants cannot completely remove these EOPs. In most cases, these EOPs are transferred to sludge due to their low solubility and high octanol/water distribution coefficient. Therefore, excess sludge is also an easy enrichment medium for these EOPs. In view of the excellent effect of non-thermal plasma in water and soil environment, it is necessary to extend this technology to the treatment of excess sludge in the future.
- (3) The positive effects of catalysts on non-thermal plasma technology have been widely recognized in a large number of studies. However, at present, the recovery of solid catalysts in soil remediation seems to be less mentioned, and the influence of catalyst residues on soil properties and microbial behavior is still in the blank stage.

## 6. Conclusions

This review provides readers with a comprehensive overview of non-thermal plasma in environmental remediation. Based on the above discussion of this review, some important conclusions can be drawn.

Firstly, the research progress of non-thermal plasma on EOPs (i.e., EDCs, PPCPs, and POPs) in different environmental media is summarized. It is found that many parameters will affect the degradation efficiency of non-thermal plasma, and it is clear from previous studies that non-thermal plasma technology shows the potential for effective degradation and complete mineralization of EOPs, which cannot be successfully removed by conventional treatment methods. For soil remediation, direct ignition of plasma discharge in the interior of soil pores seems to promote the penetration of UV and short-lived reactive species in the soil matrix, thus further promoting effective remediation of the entire porous medium.

Secondly, the generation of reactive species and the degradation mechanism of EOPs in non-thermal plasma system are discussed. Similar to other AOPs, non-thermal plasma also emphasizes that  $\bullet\text{OH}$  plays a central role in the degradation of pollutants. The degradation pathways of various EOPs are mainly the following reactions:  $\bullet\text{OH}$  is directly generated in discharge or further decomposed by  $\text{O}_3$  and  $\text{H}_2\text{O}_2$ . Then, according to the molecular structure of organic pollutants (e.g., electron density), the oxidative degradation pathway may also include the reaction with  $\text{O}_3$ .

Finally, some measures to improve the efficiency of non-thermal plasma are comprehensively summarized. In terms of water remediation, the formation of MBs under the water surface seems to have significant advantages, because it is a more effective means to provide reactive species to degrade EOPs in water and the existence of MBs enhances the

dissolution and mass transfer of reactive species generated by plasma from gas phase to liquid phase. For soil remediation, the combination of non-thermal plasma and catalyst seems to be a promising technology to break through the bottleneck of single plasma.

In conclusion, non-thermal plasma technology has a good application prospect in environmental remediation.

**Author Contributions:** All authors contributed extensively to the work presented in this paper. Y.H.: investigation, visualization, writing—original draft; W.S.: writing—review and editing; W.L.: writing—review and editing; W.Z. and C.Z.: resources; D.J.: formal analysis. All authors have read and agreed to the published version of the manuscript.

**Funding:** This work was supported by the National Natural Science Foundation of China project 51108360.

**Data Availability Statement:** Not applicable.

**Conflicts of Interest:** The authors declare no conflict of interest.

## References

1. Barbosa Ferreira, M.; Sales Solano, A.M.; Vieira Dos Santos, E.; Martínez-Huitle, C.A.; Ganiyu, S.O. Coupling of Anodic Oxidation and Soil Remediation Processes: A Review. *Materials* **2020**, *13*, 4309. [[CrossRef](#)] [[PubMed](#)]
2. Liu, J.; Ren, S.; Cao, J.; Tsang, D.C.W.; Beiyuan, J.; Peng, Y.; Fang, F.; She, J.; Yin, M.; Shen, N.; et al. Highly efficient removal of thallium in wastewater by MnFe<sub>2</sub>O<sub>4</sub>-biochar composite. *J. Hazard. Mater.* **2021**, *401*, 123311. [[CrossRef](#)] [[PubMed](#)]
3. Fu, Q.; Malchi, T.; Carter, L.J.; Li, H.; Gan, J.; Chefetz, B. Pharmaceutical and Personal Care Products: From Wastewater Treatment into Agro-Food Systems. *Environ. Sci. Technol.* **2019**, *53*, 14083–14090. [[CrossRef](#)] [[PubMed](#)]
4. Cheng, W.; Li, J.; Wu, Y.; Xu, L.; Su, C.; Qian, Y.; Zhu, Y.G.; Chen, H. Behavior of antibiotics and antibiotic resistance genes in eco-agricultural system: A case study. *J. Hazard. Mater.* **2016**, *304*, 18–25. [[CrossRef](#)]
5. Field, J.A.; Johnson, C.A.; Rose, J.B. What is “emerging”? *Environ. Sci. Technol.* **2006**, *40*, 7105. [[CrossRef](#)]
6. Liu, B.; Zhang, S.G.; Chang, C.C. Emerging pollutants—Part II: Treatment. *Water Environ. Res.* **2020**, *92*, 1603–1617. [[CrossRef](#)]
7. Ahmad, H.A.; Ahmad, S.; Cui, Q.; Wang, Z.; Wei, H.; Chen, X.; Ni, S.; Ismail, S.; Awad, H.M.; Tawfik, A. The environmental distribution and removal of emerging pollutants, highlighting the importance of using microbes as a potential degrader: A review. *Sci. Total Environ.* **2022**, *809*, 151926. [[CrossRef](#)]
8. Al-Maqdi, K.A.; Elmerhi, N.; Athamneh, K.; Bilal, M.; Alzamly, A.; Ashraf, S.S.; Shah, I. Challenges and Recent Advances in Enzyme-Mediated Wastewater Remediation—A Review. *Nanomaterials* **2021**, *11*, 3124. [[CrossRef](#)]
9. Ikehata, K.; Gamal El-Din, M.; Snyder, S.A. Ozonation and Advanced Oxidation Treatment of Emerging Organic Pollutants in Water and Wastewater. *Ozone Sci. Eng.* **2008**, *30*, 21–26. [[CrossRef](#)]
10. Cabrerizo, A.; Muir, D.C.G.; De Silva, A.O.; Wang, X.; Lamoureux, S.F.; Lafrenière, M.J. Legacy and Emerging Persistent Organic Pollutants (POPs) in Terrestrial Compartments in the High Arctic: Sorption and Secondary Sources. *Environ. Sci. Technol.* **2018**, *52*, 14187–14197. [[CrossRef](#)]
11. Ahmed, M.B.; Zhou, J.L.; Ngo, H.H.; Guo, W.; Thomaidis, N.S.; Xu, J. Progress in the biological and chemical treatment technologies for emerging contaminant removal from wastewater: A critical review. *J. Hazard. Mater.* **2016**, *323*, 274–298. [[CrossRef](#)] [[PubMed](#)]
12. Han, Y.; Yang, L.; Chen, X.; Cai, Y.; Zhang, X.; Qian, M.; Chen, X.; Zhao, H.; Sheng, M.; Cao, G.; et al. Removal of veterinary antibiotics from swine wastewater using anaerobic and aerobic biodegradation. *Sci. Total Environ.* **2020**, *709*, 136094. [[CrossRef](#)] [[PubMed](#)]
13. Zhou, L.; Liu, Z.; Guan, Z.; Tian, B.; Liu, Y. 0D/2D plasmonic Cu<sub>2</sub>-xS/g-C<sub>3</sub>N<sub>4</sub> nanosheets harnessing UV-vis-NIR broad spectrum for photocatalytic degradation of antibiotic pollutant. *Appl. Catal. B Environ.* **2019**, *263*, 118326. [[CrossRef](#)]
14. Sun, S.; Yao, H.; Li, X.; De Ng, S.; Zhang, W. Enhanced Degradation of Sulfamethoxazole (SMX) in Toilet Wastewater by Photo-Fenton Reactive Membrane Filtration. *Nanomaterials* **2020**, *10*, 180. [[CrossRef](#)] [[PubMed](#)]
15. Liu, X.; Huang, F.; He, Y.; Yu, Y.; Lv, Y.; Xu, Y.; Zhang, Y. Oxytetracycline degradation and toxicity evolution by catalytic oxidation process over sludge derived carbon. *J. Environ. Chem. Eng.* **2019**, *7*, 102889. [[CrossRef](#)]
16. Ma, J.; Jiang, Z.; Cao, J.; Yu, F. Enhanced adsorption for the removal of antibiotics by carbon nanotubes/graphene oxide/sodium alginate triple-network nanocomposite hydrogels in aqueous solutions. *Chemosphere* **2020**, *242*, 125188. [[CrossRef](#)]
17. Hernández-Abreu, A.B.; Álvarez-Torrellas, S.; Rocha, R.P.; Pereira, M.F.R.; Águeda, V.I.; Delgado, J.A.; Larriba, M.; García, J.; Figueiredo, J.L. Effective adsorption of the endocrine disruptor compound bisphenol a from water on surface-modified carbon materials. *Appl. Surf. Sci.* **2021**, *552*, 149513. [[CrossRef](#)]
18. Weng, X.; Ji, Y.; Ma, R.; Zhao, F.; An, Q.; Gao, C. Superhydrophilic and antibacterial zwitterionic polyamide nanofiltration membranes for antibiotics separation. *J. Membr. Sci.* **2016**, *510*, 122–130. [[CrossRef](#)]
19. Hao, W.; Niu, X.; Jia, Y.; Wang, C.; Lu, M. Retentions of bisphenol A and norfloxacin by three different ultrafiltration membranes in regard to drinking water treatment. *Chem. Eng. J.* **2016**, *294*, 410–416.

20. Zhang, J.; Giorno, L.; Drioli, E. Study of a hybrid process combining PACs and membrane operations for antibiotic wastewater treatment. *Desalination* **2006**, *194*, 101–107. [[CrossRef](#)]
21. Yuan, S.; Meng, T.; Lu, X. Microwave remediation of soil contaminated with hexachlorobenzene. *J. Hazard. Mater.* **2006**, *137*, 878–885. [[CrossRef](#)] [[PubMed](#)]
22. Qin, C.Y.; Zhao, Y.S.; Zheng, W.; Li, Y.S. Study on influencing factors on removal of chlorobenzene from unsaturated zone by soil vapor extraction. *J. Hazard. Mater.* **2010**, *176*, 294–299. [[CrossRef](#)] [[PubMed](#)]
23. Villa, R.D.; Trovó, A.G.; Nogueira, R.F.P. Soil remediation using a coupled process: Soil washing with surfactant followed by photo-Fenton oxidation. *J. Hazard. Mater.* **2010**, *174*, 770–775. [[CrossRef](#)] [[PubMed](#)]
24. Yeung, A.T.; Gu, Y. A review on techniques to enhance electrochemical remediation of contaminated soils. *J. Hazard. Mater.* **2011**, *195*, 11–29. [[CrossRef](#)]
25. Liao, X.; Zhao, D.; Yan, X.; Huling, S.G. Identification of persulfate oxidation products of polycyclic aromatic hydrocarbon during remediation of contaminated soil. *J. Hazard. Mater.* **2014**, *276*, 26–34. [[CrossRef](#)]
26. Kulkarni, M.; Chaudhari, A. Microbial remediation of nitro-aromatic compounds: An overview. *J. Environ. Manag.* **2007**, *85*, 496–512. [[CrossRef](#)]
27. Cao, X.; Cui, X.; Xie, M.; Zhao, R.; Xu, L.; Ni, S.; Cui, Z. Amendments and bioaugmentation enhanced phytoremediation and micro-ecology for PAHs and heavy metals co-contaminated soils. *J. Hazard. Mater.* **2022**, *426*, 128096. [[CrossRef](#)]
28. Gerrity, D.; Stanford, B.D.; Trenholm, R.A.; Snyder, S.A. An evaluation of a pilot-scale nonthermal plasma advanced oxidation process for trace organic compound degradation. *Water Res.* **2010**, *44*, 493–504. [[CrossRef](#)]
29. Bai, Y.; Chen, J.; Yang, Y.; Guo, L.; Zhang, C. Degradation of organophosphorus pesticide induced by oxygen plasma: Effects of operating parameters and reaction mechanisms. *Chemosphere* **2010**, *81*, 408–414. [[CrossRef](#)]
30. Sarangapani, C.; Danaher, M.; Tiwari, B.; Lu, P.; Bourke, P.; Cullen, P.J. Efficacy and mechanistic insights into endocrine disruptor degradation using atmospheric air plasma. *Chem. Eng. J.* **2017**, *326*, 700–714. [[CrossRef](#)]
31. Kim, K.S.; Kam, S.K.; Mok, Y.S. Elucidation of the degradation pathways of sulfonamide antibiotics in a dielectric barrier discharge plasma system. *Chem. Eng. J.* **2015**, *271*, 31–42. [[CrossRef](#)]
32. Sohrabi, A.; Haghghat, G.; Shaibani, P.M.; Van Neste, C.W.; Naicker, S.; Sadrzadeh, M.; Thundat, T. Elimination of pharmaceutical contaminants fluoxetine and propranolol by an advanced plasma water treatment. *Desalination Water Treat.* **2018**, *113*, 346–353. [[CrossRef](#)]
33. Xin, L.; Sun, Y.; Feng, J.; Wang, J.; He, D. Degradation of triclosan in aqueous solution by dielectric barrier discharge plasma combined with activated carbon fibers. *Chemosphere* **2016**, *144*, 855–863. [[CrossRef](#)] [[PubMed](#)]
34. Lei, W.; Jiang, X.; Liu, Y. Degradation of bisphenol A and formation of hydrogen peroxide induced by glow discharge plasma in aqueous solutions. *J. Hazard. Mater.* **2008**, *154*, 1106–1114.
35. Tichonovas, M.; Krugly, E.; Racys, V.; Hippler, R.; Kauneliene, V.; Stasiulaitiene, I.; Martuzevicius, D. Degradation of various textile dyes as wastewater pollutants under dielectric barrier discharge plasma treatment. *Chem. Eng. J.* **2013**, *229*, 9–19. [[CrossRef](#)]
36. Lu, N.; Wang, C.; Lou, C. Remediation of PAH-contaminated soil by pulsed corona discharge plasma. *J. Soil. Sediment.* **2017**, *17*, 97–105. [[CrossRef](#)]
37. Monica, M.; Nicolae, B.M.; Vasile, I.P. Degradation of pharmaceutical compounds in water by non-thermal plasma treatment. *Water Res.* **2015**, *81*, 124–136.
38. Russo, M.; Iervolino, G.; Vaiano, V.; Palma, V. Non-Thermal Plasma Coupled with Catalyst for the Degradation of Water Pollutants: A Review. *Catalysts* **2020**, *10*, 1438. [[CrossRef](#)]
39. Hao, Z.; Danyan, M.; Rongliang, Q.; Yetao, T.; Changming, D. Non-thermal plasma technology for organic contaminated soil remediation: A review. *Chem. Eng. J.* **2017**, *313*, 157–170.
40. Guo, H.; Wang, Y.; Liao, L.; Li, Z.; Pan, S.; Puyang, C.; Su, Y.; Zhang, Y.; Wang, T.; Ren, J.; et al. Review on remediation of organic-contaminated soil by discharge plasma: Plasma types, impact factors, plasma-assisted catalysis, and indexes for remediation. *Chem. Eng. J.* **2022**, *436*, 135239. [[CrossRef](#)]
41. Palma, D.; Richard, C.; Minella, M. State of the art and perspectives about non-thermal plasma applications for the removal of PFAS in water. *Chem. Eng. J. Adv.* **2022**, *10*, 100253.
42. Mohsen, A.; Mehdi, S.; Mohammad, H.E.; Amir, H.M.; Mohammad, H.S.; Hossein, F. Dielectric barrier discharge plasma with photocatalysts as a hybrid emerging technology for degradation of synthetic organic compounds in aqueous environments: A critical review. *Chemosphere* **2021**, *263*, 128065.
43. Hichem, Z.; Phuong, N.; Lotfi, K.; Abdeltif, A.; Aymen, A.A. Review on discharge Plasma for water treatment: Mechanism, reactor geometries, active species and combined processes. *J. Water Process Eng.* **2020**, *38*, 101664.
44. Mouele, E.S.M.; Tijani, J.O.; Badmus, K.O.; Perea, O.; Babajide, O.; Fatoba, O.O.; Zhang, C.; Shao, T.; Sosnin, E.; Tarasenko, V.; et al. A critical review on ozone and co-species, generation and reaction mechanisms in plasma induced by dielectric barrier discharge technologies for wastewater remediation. *J. Environ. Chem. Eng.* **2021**, *9*, 105758. [[CrossRef](#)]
45. Pramila, M.; Evanjalín, M.V.; Moses, J.A.; Anandharamakrishnan, C. Water decontamination using non-thermal plasma: Concepts, applications, and prospects. *J. Environ. Chem. Eng.* **2020**, *8*, 104377.
46. Gmurek, M.; Olak-Kucharczyk, M.; Ledakowicz, S. Photochemical decomposition of endocrine disrupting compounds—A review. *Chem. Eng. J.* **2017**, *310*, 437–456. [[CrossRef](#)]



47. Pal, A.; He, Y.; Jekel, M.; Reinhard, M.; Gin, Y.H. Emerging contaminants of public health significance as water quality indicator compounds in the urban water cycle. *Environ. Int.* **2014**, *71*, 46–62. [[PubMed](#)]
48. Stülten, D.; Lamshöft, M.; Zühlke, S.; Spittler, M. Isolation and characterization of a new human urinary metabolite of diclofenac applying LC–NMR–MS and high-resolution mass analyses. *J. Pharmaceut. Biomed.* **2008**, *47*, 371–376. [[CrossRef](#)]
49. Narayanan, M.; El-sheekh, M.; Ma, Y.; Pugazhendhi, A.; Natarajan, D.; Kandasamy, G.; Raja, R.; Saravana Kumar, R.M.; Kumarasamy, S.; Sathiyam, G.; et al. Current status of microbes involved in the degradation of pharmaceutical and personal care products (PPCPs) pollutants in the aquatic ecosystem. *Environ. Pollut.* **2022**, *300*, 118922.
50. Guo, M.; Feng, Y.; Li, X.; Yan, G.; Wang, X.; Li, X.; Zhang, S.; Yu, Y. Enhanced degradation of pharmaceuticals and personal care products (PPCPs) by three-dimensional electrocatalysis coupled biological aerated filter. *J. Environ. Chem. Eng.* **2021**, *9*, 106035. [[CrossRef](#)]
51. Bing, L.I.; Zhang, R. Biodegradation and adsorption of antibiotics in the activated sludge process. *Environ. Sci. Technol.* **2010**, *44*, 3468–3473.
52. Zhi, D.; Lin, Y.; Jiang, L.; Zhou, Y.; Huang, A.; Yang, J.; Luo, L. Remediation of persistent organic pollutants in aqueous systems by electrochemical activation of persulfates: A review. *J. Environ. Manag.* **2020**, *260*, 110125. [[CrossRef](#)] [[PubMed](#)]
53. Yu, J.; Zhu, Z.; Zhang, H.; Shen, X.; Qiu, Y.; Yin, D.; Wang, S. Persistent free radicals on N-doped hydrochar for degradation of endocrine disrupting compounds. *Chem. Eng. J.* **2020**, *398*, 125538. [[CrossRef](#)]
54. Maroga Mboula, V.; Héquet, V.; Andrés, Y.; Pastrana-Martínez, L.M.; Doña-Rodríguez, J.M.; Silva, A.M.T.; Falaras, P. Photocatalytic degradation of endocrine disruptor compounds under simulated solar light. *Water Res.* **2013**, *47*, 3997–4005. [[CrossRef](#)]
55. Choudhary, M.; Sarkar, P.; Kumar Sharma, S.; Kajla, A.; Neogi, S. Quantification of reactive species generated in pulsed electrical discharge plasma reactor and its application for 17 $\alpha$ -ethinylestradiol degradation in different water matrices. *Sep. Purif. Technol.* **2021**, *275*, 119173. [[CrossRef](#)]
56. Guo, H.; Jiang, N.; Li, J.; Wu, Y. Synergistic degradation of bisphenol A by pulsed discharge plasma with granular activated carbon: Effect of operating parameters, synergistic mechanism and possible degradation pathway. *Vacuum* **2018**, *156*, 402–410. [[CrossRef](#)]
57. Mao, D.; Yan, X.; Wang, H.; Shen, Z.; Yi, C. Catalysis of rGO-WO<sub>3</sub> nanocomposite for aqueous bisphenol A degradation in dielectric barrier discharge plasma oxidation process. *Chemosphere* **2020**, *262*, 128073. [[CrossRef](#)]
58. Wang, H.; Shen, Z.; Yan, X.; Guo, H.; Mao, D.; Yi, C. Dielectric barrier discharge plasma coupled with WO<sub>3</sub> for bisphenol A degradation. *Chemosphere* **2021**, *274*, 129722. [[CrossRef](#)]
59. Yang, J.; Zeng, D.; Hassan, M.; Ma, Z.; Dong, L.; Xie, Y.; He, Y. Efficient degradation of Bisphenol A by dielectric barrier discharge non-thermal plasma: Performance, degradation pathways and mechanistic consideration. *Chemosphere* **2022**, *286*, 131627. [[CrossRef](#)]
60. Wang, J.; Li, L.; Cao, H.; Yang, C.; Guo, Z.; Shi, Y.; Li, W.; Zhao, H.; Sun, J.; Xie, Y. Degradation of phenolic compounds by dielectric barrier plasma: Process optimization and influence of phenol substituents. *Chem. Eng. J.* **2020**, *385*, 123732. [[CrossRef](#)]
61. Sarangapani, C.; Misra, N.N.; Milosavljevic, V.; Bourke, P.; Cullen, P.J. Pesticide degradation in water using atmospheric air cold plasma. *J. Water Process Eng.* **2016**, *9*, 225–232. [[CrossRef](#)]
62. Wang, T.; Jia, H.; Guo, X.; Xia, T.; Qu, G.; Sun, Q.; Yin, X. Evaluation of the potential of dimethyl phthalate degradation in aqueous using sodium percarbonate activated by discharge plasma. *Chem. Eng. J.* **2018**, *346*, 65–76. [[CrossRef](#)]
63. Su, Y.; Liu, S.; Zhao, C.; Yang, X.; Liu, D. Needle electrode design of pulsed high voltage discharge reactor for performance enhancement of 4-chlorophenol degradation in highly conductive solution. *Chemosphere* **2021**, *266*, 129203. [[PubMed](#)]
64. Guo, H.; Jiang, N.; Wang, H.; Lu, N.; Shang, K.; Li, J.; Wu, Y. Pulsed discharge plasma assisted with graphene-WO<sub>3</sub> nanocomposites for synergistic degradation of antibiotic enrofloxacin in water. *Chem. Eng. J.* **2019**, *372*, 226–240.
65. Tang, S.; Yuan, D.; Rao, Y.; Li, N.; Qi, J.; Cheng, T.; Sun, Z.; Gu, J.; Huang, H. Persulfate activation in gas phase surface discharge plasma for synergetic removal of antibiotic in water. *Chem. Eng. J.* **2018**, *337*, 446–454. [[CrossRef](#)]
66. Hu, X.; Wang, B. Removal of pefloxacin from wastewater by dielectric barrier discharge plasma: Mechanism and degradation pathways. *J. Environ. Chem. Eng.* **2021**, *9*, 105720. [[CrossRef](#)]
67. Shoufeng, T.A.N.G.; Xue, L.I.; Zhang, C.; Yang, L.I.U.; Zhang, W.; Deling, Y.U.A.N. Strengthening decomposition of oxytetracycline in DBD plasma coupling with Fe-Mn oxide-loaded granular activated carbon. *Plasma Sci. Technol.* **2019**, *21*, 25504.
68. Ansari, M.; Hossein Mahvi, A.; Hossein Salmani, M.; Sharifian, M.; Fallahzadeh, H.; Hassan Ehrampoush, M. Dielectric barrier discharge plasma combined with nano catalyst for aqueous amoxicillin removal: Performance modeling, kinetics and optimization study, energy yield, degradation pathway, and toxicity. *Sep. Purif. Technol.* **2020**, *251*, 117270. [[CrossRef](#)]
69. Guo, H.; Li, Z.; Zhang, Y.; Jiang, N.; Wang, H.; Li, J. Degradation of chloramphenicol by pulsed discharge plasma with heterogeneous Fenton process using Fe<sub>3</sub>O<sub>4</sub> nanocomposites. *Sep. Purif. Technol.* **2020**, *253*, 117540. [[CrossRef](#)]
70. Lou, J.; Wei, Y.; Zhang, M.; Meng, Q.; Jia, M. Removal of tetracycline hydrochloride in aqueous by coupling dielectric barrier discharge plasma with biochar. *Sep. Purif. Technol.* **2021**, *266*, 118515. [[CrossRef](#)]
71. Guo, H.; Li, Z.; Xie, Z.; Song, J.; Wang, H. Accelerated Fenton reaction for antibiotic ofloxacin degradation in discharge plasma system based on graphene-Fe<sub>3</sub>O<sub>4</sub> nanocomposites. *Vacuum* **2020**, *185*, 110022. [[CrossRef](#)]
72. Guo, H.; Wang, Y.; Yao, X.; Zhang, Y.; Wang, H. A comprehensive insight into plasma-catalytic removal of antibiotic oxytetracycline based on graphene-TiO<sub>2</sub>-Fe<sub>3</sub>O<sub>4</sub> nanocomposites. *Chem. Eng. J.* **2021**, *425*, 130614. [[CrossRef](#)]

73. Zhang, G.; Sun, Y.; Zhang, C.; Yu, Z. Decomposition of acetaminophen in water by a gas phase dielectric barrier discharge plasma combined with TiO<sub>2</sub>-rGO nanocomposite: Mechanism and degradation pathway. *J. Hazard. Mater.* **2017**, *323*, 719–729. [[CrossRef](#)]
74. Hama Aziz, K.H.; Miessner, H.; Mueller, S.; Kalass, D.; Moeller, D.; Khorshid, I.; Rashid, M.A.M. Degradation of pharmaceutical diclofenac and ibuprofen in aqueous solution, a direct comparison of ozonation, photocatalysis, and non-thermal plasma. *Chem. Eng. J.* **2017**, *313*, 1033–1041. [[CrossRef](#)]
75. Magureanu, M.; Mandache, N.B.; Bradu, C.; Parvulescu, V.I. High efficiency plasma treatment of water contaminated with organic compounds. Study of the degradation of ibuprofen. *Plasma Process. Polym.* **2018**, *15*, 1700201. [[CrossRef](#)]
76. Zheng, B.; Li, C.; Zhang, J.; Zheng, Z. Dielectric barrier discharge induced the degradation of the emerging contaminant ibuprofen in aqueous solutions. *Desalin. Water Treat.* **2014**, *52*, 4469–4475. [[CrossRef](#)]
77. Banaschik, R.; Jablonowski, H.; Bednarski, P.J.; Kolb, J.F. Degradation and intermediates of diclofenac as instructive example for decomposition of recalcitrant pharmaceuticals by hydroxyl radicals generated with pulsed corona plasma in water. *J. Hazard. Mater.* **2018**, *342*, 651–660. [[CrossRef](#)]
78. Magureanu, M.; Piroi, D.; Mandache, N.B.; David, V.; Medvedovici, A.; Bradu, C.; Parvulescu, V.I. Degradation of antibiotics in water by non-thermal plasma treatment. *Water Res.* **2011**, *45*, 3407–3416. [[CrossRef](#)]
79. Dobrin, D.; Bradu, C.; Magureanu, M.; Mandache, N.B.; Parvulescu, V.I. Degradation of diclofenac in water using a pulsed corona discharge. *Chem. Eng. J.* **2013**, *234*, 389–396. [[CrossRef](#)]
80. Magureanu, M.; Dobrin, D.; Mandache, N.B.; Bradu, C.; Medvedovici, A.; Parvulescu, V.I. The Mechanism of Plasma Destruction of Enalapril and Related Metabolites in Water. *Plasma Process. Polym.* **2013**, *10*, 459–468. [[CrossRef](#)]
81. Korichi, N.; Aubry, O.; Rabat, H.; Cagnon, B.; Hong, D. Paracetamol Degradation by Catalyst Enhanced Non-Thermal Plasma Process for a Drastic Increase in the Mineralization Rate. *Catalysts* **2020**, *10*, 959. [[CrossRef](#)]
82. Krishna, S.; Ceriani, E.; Marotta, E.; Giardina, A.; Špatenka, P.; Paradisi, C. Products and mechanism of verapamil removal in water by air non-thermal plasma treatment. *Chem. Eng. J.* **2016**, *292*, 35–41. [[CrossRef](#)]
83. Lee, H.; Park, Y.; Kim, J.; Park, Y.; Jung, S. Degradation of dimethyl phthalate using a liquid phase plasma process with TiO<sub>2</sub> photocatalysts. *Environ. Res.* **2019**, *169*, 256–260. [[CrossRef](#)] [[PubMed](#)]
84. Bratty, M.A.; Al-Rajab, A.J.; Rehman, Z.U.; Sharma, M.; Alhazmi, H.A.; Najmi, A.; Muzafar, H.; Javed, S.A. Fast and efficient removal of caffeine from water using dielectric barrier discharge. *Appl. Water Sci.* **2021**, *11*, 1–10. [[CrossRef](#)]
85. Wang, J.; Sun, Y.; Jiang, H.; Feng, J. Removal of caffeine from water by combining dielectric barrier discharge (DBD) plasma with goethite. *J. Saudi Chem. Soc.* **2017**, *21*, 545–557. [[CrossRef](#)]
86. Wang, L.; Sun, L.; Yu, Z.; Hou, Y.; Peng, Z.; Yang, F.; Chen, Y.; Huang, J. Synergetic decomposition performance and mechanism of perfluorooctanoic acid in dielectric barrier discharge plasma system with Fe<sub>3</sub>O<sub>4</sub>@SiO<sub>2</sub>-BiOBr magnetic photocatalyst. *Mol. Catal.* **2017**, *441*, 179–189. [[CrossRef](#)]
87. Corella Puertas, E.; Peyot, M.; Pineda, M.; Volk, K.; Coulombe, S.; Yargeau, V. Degradation of diatrizoate in a pin-to-liquid plasma reactor, its transformation products and their residual toxicity. *Sci. Total Environ.* **2021**, *782*, 146895. [[CrossRef](#)]
88. Magureanu, M.; Piroi, D.; Mandache, N.B.; David, V.; Medvedovici, A.; Parvulescu, V.I. Degradation of pharmaceutical compound pentoxifylline in water by non-thermal plasma treatment. *Water Res.* **2010**, *44*, 3445–3453. [[CrossRef](#)]
89. Huang, Q.; Fang, C. Degradation of 3,3',4,4'-tetrachlorobiphenyl (PCB77) by dielectric barrier discharge (DBD) non-thermal plasma: Degradation mechanism and toxicity evaluation. *Sci. Total Environ.* **2020**, *739*, 139926. [[CrossRef](#)]
90. Sahni, M.; Finney, W.C.; Locke, B.R. Degradation of aqueous phase polychlorinated biphenyls (PCB) using pulsed corona discharges. *J. Adv. Oxid. Technol.* **2005**, *8*, 105–111. [[CrossRef](#)]
91. Aggelopoulos, C.A.; Merpoulis, S.; Hatzisymeon, M.; Lada, Z.G.; Rassias, G. Degradation of antibiotic enrofloxacin in water by gas-liquid nsp-DBD plasma: Parametric analysis, effect of H<sub>2</sub>O<sub>2</sub> and CaO<sub>2</sub> additives and exploration of degradation mechanisms. *Chem. Eng. J.* **2020**, *398*, 125622. [[CrossRef](#)]
92. Ruan, J.J.; Li, W.; Shi, Y.; Nie, Y.; Wang, X.; Tan, T.E. Decomposition of simulated odors in municipal wastewater treatment plants by a wire-plate pulse corona reactor. *Chemosphere* **2005**, *59*, 327–333. [[CrossRef](#)] [[PubMed](#)]
93. Jiang, N.; Lu, N.; Shang, K.; Li, J.; Wu, Y. Effects of electrode geometry on the performance of dielectric barrier/packed-bed discharge plasmas in benzene degradation. *J. Hazard. Mater.* **2013**, *262*, 387–393. [[CrossRef](#)] [[PubMed](#)]
94. Joshi, R.P.; Thagard, S.M. Streamer-Like Electrical Discharges in Water: Part II. Environmental Applications. *Plasma Chem. Plasma Process.* **2013**, *33*, 17–49. [[CrossRef](#)]
95. Bing, S.; Sato, M.; Clements, J.S. Optical study of active species produced by a pulsed streamer corona discharge in water. *J. Electrostat.* **1997**, *39*, 189–202.
96. Lukes, P.; Dolezalova, E.; Sisrova, I.; Clupek, M. Aqueous-phase chemistry and bactericidal effects from an air discharge plasma in contact with water: Evidence for the formation of peroxyxynitrite through a pseudo-second-order post-discharge reaction of H<sub>2</sub>O<sub>2</sub> and HNO<sub>2</sub>. *Plasma Sources Sci. Technol.* **2014**, *23*, 15019. [[CrossRef](#)]
97. Li, H.; Li, T.; He, S.; Zhou, J.; Wang, T.; Zhu, L. Efficient degradation of antibiotics by non-thermal discharge plasma: Highlight the impacts of molecular structures and degradation pathways. *Chem. Eng. J.* **2020**, *395*, 125091. [[CrossRef](#)]
98. Singh, R.K.; Philip, L.; Ramanujam, S. Rapid degradation, mineralization and detoxification of pharmaceutically active compounds in aqueous solution during pulsed corona discharge treatment. *Water Res.* **2017**, *121*, 20–36. [[CrossRef](#)]
99. Wang, T.; Lu, N.; Li, J.; Wu, Y.; Su, Y. Enhanced degradation of p-nitrophenol in soil in a pulsed discharge plasma-catalytic system. *J. Hazard. Mater.* **2011**, *195*, 276–280. [[CrossRef](#)]



100. Wang, T.; Ren, J.; Qu, G.; Liang, D.; Hu, S. Glyphosate contaminated soil remediation by atmospheric pressure dielectric barrier discharge plasma and its residual toxicity evaluation. *J. Hazard. Mater.* **2016**, *320*, 539–546. [[CrossRef](#)]
101. Aggelopoulos, C.A.; Tataraki, D.; Rassias, G. Degradation of atrazine in soil by dielectric barrier discharge plasma—Potential singlet oxygen mediation. *Chem. Eng. J.* **2018**, *347*, 682–694. [[CrossRef](#)]
102. Wang, T.C.; Lu, N.; Li, J.; Wu, Y. Degradation of pentachlorophenol in soil by pulsed corona discharge plasma. *J. Hazard. Mater.* **2010**, *180*, 436–441. [[CrossRef](#)] [[PubMed](#)]
103. Wang, T.C.; Qu, G.; Li, J.; Liang, D. Remediation of p-nitrophenol and pentachlorophenol mixtures contaminated soil using pulsed corona discharge plasma. *Sep. Purif. Technol.* **2014**, *122*, 17–23. [[CrossRef](#)]
104. Hatzisymeon, M.; Tataraki, D.; Rassias, G.; Aggelopoulos, C.A. Novel combination of high voltage nanopulses and in-soil generated plasma micro-discharges applied for the highly efficient degradation of trifluralin. *J. Hazard. Mater.* **2021**, *415*, 125646. [[CrossRef](#)] [[PubMed](#)]
105. Lou, J.; Lu, N.; Li, J.; Wang, T.; Wu, Y. Remediation of chloramphenicol-contaminated soil by atmospheric pressure dielectric barrier discharge. *Chem. Eng. J.* **2012**, *180*, 99–105. [[CrossRef](#)]
106. Aggelopoulos, C.A.; Hatzisymeon, M.; Tataraki, D.; Rassias, G. Remediation of ciprofloxacin-contaminated soil by nanosecond pulsed dielectric barrier discharge plasma: Influencing factors and degradation mechanisms. *Chem. Eng. J.* **2020**, *393*, 124768. [[CrossRef](#)]
107. Hatzisymeon, M.; Tataraki, D.; Tsakiroglou, C.; Rassias, G.; Aggelopoulos, C.A. Highly energy-efficient degradation of antibiotics in soil: Extensive cold plasma discharges generation in soil pores driven by high voltage nanopulses. *Sci. Total Environ.* **2021**, *786*, 147420. [[CrossRef](#)]
108. Mu, R.; Liu, Y.; Li, R.; Xue, G.; Ognier, S. Remediation of pyrene-contaminated soil by active species generated from flat-plate dielectric barrier discharge. *Chem. Eng. J.* **2016**, *296*, 356–365. [[CrossRef](#)]
109. Zhan, J.; Liu, Y.; Cheng, W.; Zhang, A.; Li, R.; Li, X.; Ognier, S.; Cai, S.; Yang, C.; Liu, J. Remediation of soil contaminated by fluorene using needle-plate pulsed corona discharge plasma. *Chem. Eng. J.* **2018**, *334*, 2124–2133. [[CrossRef](#)]
110. Abbas, Y.; Lu, W.; Dai, H.; Fu, X.; Ye, R.; Wang, H. Remediation of polycyclic aromatic hydrocarbons (PAHs) contaminated soil with double dielectric barrier discharge plasma technology: Influencing parameters. *Chem. Eng. J.* **2020**, *394*, 124858. [[CrossRef](#)]
111. Abbas, Y.; Lu, W.; Wang, Q.; Dai, H.; Liu, Y.; Fu, X.; Pan, C.; Ghaedi, H.; Cheng, F.; Wang, H. Remediation of pyrene contaminated soil by double dielectric barrier discharge plasma technology: Performance optimization and evaluation. *Environ. Pollut.* **2020**, *260*, 113944. [[CrossRef](#)] [[PubMed](#)]
112. Li, R.; Liu, Y.; Cheng, W.; Zhang, W.; Xue, G.; Ognier, S. Study on remediation of phenanthrene contaminated soil by pulsed dielectric barrier discharge plasma: The role of active species. *Chem. Eng. J.* **2016**, *296*, 132–140. [[CrossRef](#)]
113. Li, X.; Zhang, H.; Luo, Y.; Teng, Y. Remediation of soil heavily polluted with polychlorinated biphenyls using a low-temperature plasma technique. *Front. Environ. Sci. Eng.* **2014**, *8*, 277–283. [[CrossRef](#)]
114. Shu, Z.; Lin, Z.; Yue, L.; Wang, W.; Wang, X. Modeling of the production of OH and O radicals in a positive pulsed corona discharge plasma. *Vacuum* **2008**, *83*, 238–243.
115. Hsu, I.Y.; Masten, S.J. The Kinetics of the Reaction of Ozone with Phenanthrene in Unsaturated Soils. *Environ. Eng. Sci.* **1997**, *14*, 207–218. [[CrossRef](#)]
116. Laroussi, M.; Lu, X.; Kolobov, V.; Arslanbekov, R. Power consideration in the pulsed dielectric barrier discharge at atmospheric pressure. *J. Appl. Phys.* **2004**, *96*, 3028–3030. [[CrossRef](#)]
117. Mildren, R.P.; Carman, R.J. Enhanced performance of a dielectric barrier discharge lamp using short-pulsed excitation. *J. Phys. D Appl. Phys.* **2001**, *34*, L1–L6. [[CrossRef](#)]
118. Walsh, J.L.; Kong, M.G. 10 ns pulsed atmospheric air plasma for uniform treatment of polymeric surfaces. *Appl. Phys. Lett.* **2007**, *91*, 1539. [[CrossRef](#)]
119. Jiang, H.; Shao, T.; Zhang, C.; Niu, Z.; Yu, Y.; Yan, P.; Zhou, Y. Comparison of AC and Nanosecond-Pulsed DBDs in Atmospheric Air. *IEEE Trans. Plasma Sci.* **2011**, *39*, 2076–2077. [[CrossRef](#)]
120. Williamson, J.M.; Trump, D.D.; Bletzinger, P.; Ganguly, B.N. Comparison of high-voltage ac and pulsed operation of a surface dielectric barrier discharge. *J. Phys. D Appl. Phys.* **2006**, *39*, 4400–4406. [[CrossRef](#)]
121. Hama Aziz, K.H.; Miessner, H.; Mueller, S.; Mahyar, A.; Kalass, D.; Moeller, D.; Khorshid, I.; Rashid, M.A.M. Comparative study on 2,4-dichlorophenoxyacetic acid and 2,4-dichlorophenol removal from aqueous solutions via ozonation, photocatalysis and non-thermal plasma using a planar falling film reactor. *J. Hazard. Mater.* **2018**, *343*, 107–115. [[CrossRef](#)] [[PubMed](#)]
122. Li, Z.; Wang, Y.; Guo, H.; Pan, S.; Puyang, C.; Su, Y.; Qiao, W.; Han, J. Insights into water film DBD plasma driven by pulse power for ibuprofen elimination in water: Performance, mechanism and degradation route. *Sep. Purif. Technol.* **2021**, *277*, 119415. [[CrossRef](#)]
123. Hoigné, J.; Bader, H. Rate constants of reactions of ozone with organic and inorganic compounds in water—II: Dissociating organic compounds. *Water Res.* **1983**, *17*, 185–194. [[CrossRef](#)]
124. Zhang, Y.; Han, C.; Zhang, G.; Dionysiou, D.D.; Nadagouda, M.N. PEG-assisted synthesis of crystal TiO<sub>2</sub> nanowires with high specific surface area for enhanced photocatalytic degradation of atrazine. *Chem. Eng. J.* **2015**, *268*, 170–179. [[CrossRef](#)]
125. Bruggeman, P.; Schram, D.C. On OH production in water containing atmospheric pressure plasmas. *Plasma Sources Sci. Technol.* **2010**, *19*, 45025–45033. [[CrossRef](#)]

126. Kogelschatz, U. Dielectric-Barrier Discharges: Their History, Discharge Physics, and Industrial Applications. *Plasma Chem. Plasma Process.* **2003**, *23*, 1–46. [[CrossRef](#)]
127. Locke, B.R.; Shih, K. Review of the methods to form hydrogen peroxide in electrical discharge plasma with liquid water. *Plasma Sources Sci. Technol.* **2011**, *20*, 34006. [[CrossRef](#)]
128. Zahran, E.M.; Bhattacharyya, D.; Bachas, L.G. Reactivity of Pd/Fe bimetallic nanotubes in dechlorination of coplanar polychlorinated biphenyls. *Chemosphere* **2013**, *91*, 165–171. [[CrossRef](#)]
129. Zhang, H.; Zhang, Q.; Miao, C.; Huang, Q. Degradation of 2, 4-dichlorophenol in aqueous solution by dielectric barrier discharge: Effects of plasma-working gases, degradation pathways and toxicity assessment. *Chemosphere* **2018**, *204*, 351–358. [[CrossRef](#)]
130. Zhang, Q.; Zhang, H.; Zhang, Q.; Huang, Q. Degradation of norfloxacin in aqueous solution by atmospheric-pressure non-thermal plasma: Mechanism and degradation pathways. *Chemosphere* **2018**, *210*, 433–439. [[CrossRef](#)]
131. Dudita, M.; Bogatu, C.; Enesca, A.; Duta, A. The influence of the additives composition and concentration on the properties of SnO<sub>x</sub> thin films used in photocatalysis. *Mater. Lett.* **2011**, *65*, 2185–2189. [[CrossRef](#)]
132. Rafieenia, R.; Sulonen, M.; Mahmoud, M.; El-Gohary, F.; Rossa, C.A. Integration of microbial electrochemical systems and photocatalysis for sustainable treatment of organic recalcitrant wastewaters: Main mechanisms, recent advances, and present prospects. *Sci. Total Environ.* **2022**, *824*, 153923. [[CrossRef](#)]
133. Wu, J.; Xiong, Q.; Liang, J.; He, Q.; Yang, D.; Deng, R.; Chen, Y. Degradation of benzotriazole by DBD plasma and peroxymonosulfate: Mechanism, degradation pathway and potential toxicity. *Chem. Eng. J.* **2020**, *384*, 123300. [[CrossRef](#)]
134. Shang, K.; Wang, X.; Li, J.; Wang, H.; Lu, N.; Jiang, N.; Wu, Y. Synergetic degradation of Acid Orange 7 (AO7) dye by DBD plasma and persulfate. *Chem. Eng. J.* **2017**, *311*, 378–384. [[CrossRef](#)]
135. Wang, X.; Wang, P.; Liu, X.; Hu, L.; Wang, Q.; Xu, P.; Zhang, G. Enhanced degradation of PFOA in water by dielectric barrier discharge plasma in a coaxial cylindrical structure with the assistance of peroxymonosulfate. *Chem. Eng. J.* **2020**, *389*, 124381. [[CrossRef](#)]
136. Liang, J.; Zhou, X.; Zhao, Z.; Yang, D.; Wang, W. Degradation of trimethoprim in aqueous by persulfate activated with nanosecond pulsed gas-liquid discharge plasma. *J. Environ. Manag.* **2021**, *278*, 111539. [[CrossRef](#)]
137. Tang, S.; Yuan, D.; Rao, Y.; Li, M.; Shi, G.; Gu, J.; Zhang, T. Percarbonate promoted antibiotic decomposition in dielectric barrier discharge plasma. *J. Hazard. Mater.* **2019**, *366*, 669–676. [[CrossRef](#)]
138. Xu, Z.; Xue, X.; Hu, S.; Li, Y.; Shen, J.; Lan, Y.; Zhou, R.; Yang, F.; Cheng, C. Degradation effect and mechanism of gas-liquid phase dielectric barrier discharge on norfloxacin combined with H<sub>2</sub>O<sub>2</sub> or Fe<sup>2+</sup>. *Sep. Purif. Technol.* **2020**, *230*, 115862. [[CrossRef](#)]
139. Sang, W.; Lu, W.; Mei, L.; Jia, D.; Cao, C.; Li, Q.; Wang, C.; Zhan, C.; Li, M. Research on different oxidants synergy with dielectric barrier discharge plasma in degradation of Orange G: Efficiency and mechanism. *Sep. Purif. Technol.* **2021**, *277*, 119473. [[CrossRef](#)]
140. Chen, J.; Feng, J.; Lu, S.; Shen, Z.; Du, Y.; Peng, L.; Nian, P.; Yuan, S.; Zhang, A. Non-thermal plasma and Fe<sup>2+</sup> activated persulfate ignited degradation of aqueous crystal violet: Degradation mechanism and artificial neural network modeling. *Sep. Purif. Technol.* **2018**, *191*, 75–85. [[CrossRef](#)]
141. Koprivanac, N.; Kusi, H.; Vujevi, D.; Peternel, I.; Locke, B.R. Influence of iron on degradation of organic dyes in corona. *J. Hazard. Mater.* **2005**, *117*, 113–119. [[CrossRef](#)] [[PubMed](#)]
142. Hao, X.; Zhou, M.; Xin, Q.; Lei, L. Pulsed discharge plasma induced Fenton-like reactions for the enhancement of the degradation of 4-chlorophenol in water. *Chemosphere* **2007**, *66*, 2185–2192. [[CrossRef](#)] [[PubMed](#)]
143. Zhou, R.; Zhou, R.; Zhang, X.; Tu, S.; Yin, Y.; Yang, S.; Ye, L. An efficient bio-adsorbent for the removal of dye: Adsorption studies and cold atmospheric plasma regeneration. *J. Taiwan Inst. Chem. Eng.* **2016**, *68*, 372–378. [[CrossRef](#)]
144. Cheng, J.; Wang, D.; Wang, B.; Ning, H.; Zhang, Y.; Li, Y.; An, J.; Gao, P. Plasma-catalytic degradation of ciprofloxacin in aqueous solution over different MnO<sub>2</sub> nanocrystals in a dielectric barrier discharge system. *Chemosphere* **2020**, *253*, 126595. [[CrossRef](#)] [[PubMed](#)]
145. Ghezzar, M.R.; Abdelmalek, F.; Belhadj, M.; Benderdouche, N.; Addou, A. Enhancement of the bleaching and degradation of textile wastewaters by Gliding arc discharge plasma in the presence of TiO<sub>2</sub> catalyst. *J. Hazard. Mater.* **2009**, *164*, 1266–1274. [[CrossRef](#)] [[PubMed](#)]
146. Jögi, I.; Erme, K.; Raud, J.; Raud, S. The Effect of TiO<sub>2</sub> Catalyst on Ozone and Nitrous Oxide Production by Dielectric Barrier Discharge. *Catal. Lett.* **2020**, *150*, 992–997. [[CrossRef](#)]
147. Guo, H.; Jiang, N.; Wang, H.; Shang, K.; Lu, N.; Li, J.; Wu, Y. Enhanced catalytic performance of graphene-TiO<sub>2</sub> nanocomposites for synergetic degradation of fluoroquinolone antibiotic in pulsed discharge plasma system. *Appl. Catal. B Environ.* **2019**, *248*, 552–566. [[CrossRef](#)]
148. Wang, B.; Wang, C.; Yao, S.; Peng, Y.; Xu, Y. Plasma-catalytic degradation of tetracycline hydrochloride over Mn/γ-Al<sub>2</sub>O<sub>3</sub> catalysts in a dielectric barrier discharge reactor. *Plasma Sci. Technol.* **2019**, *21*, 65503. [[CrossRef](#)]
149. Wang, T.C.; Lu, N.; Li, J.; Wu, Y. Plasma-TiO<sub>2</sub> catalytic method for high-efficiency remediation of p-nitrophenol contaminated soil in pulsed discharge. *Environ. Sci. Technol.* **2011**, *45*, 9301. [[CrossRef](#)]
150. Sohrabi, M.R.; Ghavami, M. Photocatalytic degradation of Direct Red 23 dye using UV/TiO<sub>2</sub>: Effect of operational parameters. *J. Hazard. Mater.* **2008**, *153*, 1235–1239. [[CrossRef](#)]
151. Takahashi, M. ζ Potential of Microbubbles in Aqueous Solutions: Electrical Properties of the Gas–Water Interface. *J. Phys. Chem. B* **2005**, *109*, 21858–21864. [[CrossRef](#)] [[PubMed](#)]

152. Takahashi, M.; Chiba, K.; Li, P. Free-radical generation from collapsing microbubbles in the absence of a dynamic stimulus. *J. Phys. Chem. B* **2007**, *111*, 1343–1347. [[CrossRef](#)] [[PubMed](#)]
153. Li, P.; Takahashi, M.; Chiba, K. Enhanced free-radical generation by shrinking microbubbles using a copper catalyst. *Chemosphere* **2009**, *77*, 1157–1160. [[CrossRef](#)] [[PubMed](#)]
154. Liu, Y.; Shen, X.; Sun, J.; Li, P.; Zhang, A. Treatment of aniline contaminated water by a self-designed dielectric barrier discharge reactor coupling with micro-bubbles: Optimization of the system and effects of water matrix. *J. Chem. Technol. Biotechnol.* **2019**, *94*, 494–504. [[CrossRef](#)]
155. Liu, Y.; Zhang, H.; Sun, J.; Liu, J.; Shen, X.; Zhan, J.; Zhang, A.; Ognier, S.; Cavadias, S.; Li, P. Degradation of aniline in aqueous solution using non-thermal plasma generated in microbubbles. *Chem. Eng. J.* **2018**, *345*, 679–687. [[CrossRef](#)]
156. Zhang, H.; Li, P.; Zhang, A.; Sun, Z.; Liu, J.; Héroux, P.; Liu, Y. Enhancing Interface Reactions by Introducing Microbubbles into a Plasma Treatment Process for Efficient Decomposition of PFOA. *Environ. Sci. Technol.* **2021**, *55*, 16067–16077. [[CrossRef](#)]
157. Wang, Q.; Zhang, A.; Li, P.; Héroux, P.; Zhang, H.; Yu, X.; Liu, Y. Degradation of aqueous atrazine using persulfate activated by electrochemical plasma coupling with microbubbles: Removal mechanisms and potential applications. *J. Hazard. Mater.* **2021**, *403*, 124087. [[CrossRef](#)]